

000 001 002 003 004 005 006 007 008 009 010 011 012 013 014 015 016 017 018 019 020 021 022 023 024 025 026 027 028 029 030 031 032 033 034 035 036 037 038 039 040 041 042 043 044 045 046 047 048 049 050 051 052 053 COMPODISTILL: ATTENTION DISTILLATION FOR COMPOSITIONAL REASONING IN MULTIMODAL LLMs

Anonymous authors

Paper under double-blind review

ABSTRACT

Recently, efficient Multimodal Large Language Models (MLLMs) have gained significant attention as a solution to their high computational complexity, making them more practical for real-world applications. In this regard, the knowledge distillation (KD) approach has emerged as a promising alternative, which transfers the rich visual and linguistic knowledge from a larger model (teacher) to a smaller model (student). However, we observe that existing KD methods struggle to effectively distill the teacher MLLM's rich *visual perception* abilities to the student, a challenge that has been largely overlooked in previous studies. Through a systematic analysis, we identify visual attention misalignment between student and teacher as the main cause of this issue. Based on this insight, we propose **CompoDistill**, a novel KD framework that explicitly aligns the student's visual attention with that of the teacher to enhance the student's visual perception abilities. Our extensive experiments show that **CompoDistill** significantly improves performance on compositional reasoning tasks that require visual perception abilities while maintaining strong performance on visual question answering tasks, as done in existing studies. Furthermore, **CompoDistill** demonstrates effectiveness with a more advanced backbone, highlighting its generalizability.

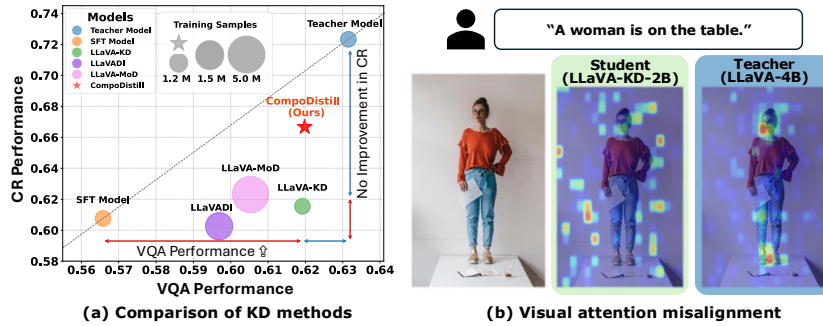


Figure 1: (a) Comparison of the teacher (LLaVA-4B), SFT (LLaVA-2B), and various 2B KD methods distilled from the same teacher. (b) *Visual attention misalignment* between the student (LLaVA-KD-2B) and teacher (LLaVA-4B), where the student attends to irrelevant image regions for the text query *A woman is on the table*, in contrast to the teacher. For more examples including our proposed method, **CompoDistill**, please refer to Appendix A.

1 INTRODUCTION

Multimodal Large Language Models (MLLMs) (Liu et al., 2023; Lin et al., 2024b) have demonstrated superior performance on various vision-language tasks over vision-language models (Radford et al., 2021; Zhai et al., 2023), marking a significant step forward in multimodal learning. Yet, their advancement has largely been driven by scaling laws, which has resulted in ever-larger and more computationally demanding architectures (OpenAI, 2023; Qwen et al., 2025). The substantial computational and memory costs associated with such massive models pose considerable challenges for practical deployment. This has, in turn, intensified interest in developing **efficient MLLMs** that can maintain strong multimodal capabilities while mitigating resource requirements.

To this end, **knowledge distillation (KD)** (Cai et al., 2024; Shu et al., 2024; Xu et al., 2024) has emerged as a promising approach, transferring rich knowledge from a larger *teacher* model to a smaller *student* model. These KD-based methods have demonstrated effectiveness in visual question

054 answering (VQA) tasks (e.g., GQA (Hudson & Manning, 2019)), which require *visual recognition*
 055 ability, outperforming the standard supervised fine-tuning (SFT model¹ in Figure 1(a)).
 056

057 Despite the progress of KD methods in visual recognition ability, a crucial question remains unex-
 058 plored: *Is visual perception ability equally well distilled?* *Visual recognition* refers to tasks like
 059 object classification, where the goal is to identify objects in images based on their features. On the
 060 other hand, *Visual perception* involves more complex abilities, such as understanding relationships
 061 among objects and accurately capturing their attributes—capabilities essential for real-world mul-
 062 timodal applications². To answer the question, in Figure 1(a), we compare the state-of-the-art KD
 063 methods (Shu et al., 2024; Cai et al., 2024; Xu et al., 2024) on VQA and compositional reasoning
 064 (CR) datasets, where VQA serves as a benchmark for evaluating visual recognition ability and CR
 065 is designed to assess visual perception ability³. We observe that, although existing KD methods
 066 show significant performance improvements on the VQA, their performance on the CR is on par
 067 with the SFT model, which is unexpected. Based on this observation, *we argue that existing KD*
methods struggle to effectively distill visual perception ability from the teacher model.

068 Beyond a simple performance comparison, we investigate the failure of the existing KD methods in
 069 distilling visual perception ability and analyze the attention maps of both the student (i.e., LLaVA-
 070 KD-2B (Cai et al., 2024)) and the teacher (i.e., LLaVA-4B (Liu et al., 2023)) models. Specifically,
 071 by visualizing their focus areas for a given text, we aim to identify differences in attention, which
 072 we believe are closely related to perception ability. As shown in Figure 1(b), we observe that the
 073 student model struggles to focus on the relevant regions, while the teacher model captures them ef-
 074 fectively, revealing a clear mismatch in the attention distributions between the teacher and the student
 075 models. The discrepancy in attention distributions, which we term *visual attention misalignment*,
 076 reveals that although KD methods aim to transfer knowledge from the teacher to the student through
 077 knowledge distillation, the student fails to inherit the teacher’s powerful visual attention mechanism,
 thereby limiting the effective distillation of visual perception ability.

078 In this regard, we hypothesize that the limited performance improvement of KD methods in CR
 079 tasks arises from the visual attention misalignment between the teacher and student models. To
 080 empirically validate our hypothesis, we conduct controlled experiments examining the relationship
 081 between attention behavior and visual task performance in Section 3. Our results demonstrate that
 082 this misalignment is directly responsible for the unexpectedly low performance of the existing KD
 083 methods in CR tasks, and this study is the first to establish that addressing visual attention misalign-
 084 ment is the key to enhancing the student model’s visual perception ability.

085 Motivated by these findings, we propose **CompoDistill**, a novel KD framework aimed at effectively
 086 distilling the teacher’s rich visual perception abilities to the student model by addressing visual
 087 attention misalignment. We introduce the **Visual ATtention alignment (VAT)** module to explicit
 088 align the visual attention of the student model with that of the teacher model, using a simple yet
 089 effective group matching strategy, in which each student layer is matched with a group of teacher
 090 layers in a one-to-many manner, to handle the difference in the number of LLM layers between the
 091 teacher and student. However, the teacher’s visual attention is optimized for its own vision-language
 092 space, making a simple transfer via the VAT module ineffective within the student’s distinct and
 093 incompatible space. This mismatch creates a conflict between the student’s feature space and the
 094 imposed attention mechanism, ultimately restricting the model’s inherent perceptual abilities. To
 095 this end, we propose the **Teacher Adapter Fetch (TAF)** module to bridge this feature space gap and
 096 enable synergy with the VAT module. Building on this, we introduce a meticulously designed three-
 097 stage training strategy that leverages both modules to comprehensively distill visual perception.

098 Through extensive experiments on multiple CR datasets, we demonstrate that **CompoDistill** sig-
 099 nificantly outperforms existing KD methods, demonstrating the effectiveness of **CompoDistill** in
 100 enhancing the student model’s visual perception ability. Meanwhile, **CompoDistill** maintains com-
 101 petitive performance on VQA datasets, preserving its visual recognition abilities. Furthermore, we
 102 demonstrate the effectiveness of **CompoDistill** with a more advanced backbone, highlighting its
 103 generalizability.

104 ¹Sharing the same architecture and size as the student models in KD, this model is trained only with visual
 105 instruction tuning Liu et al. (2023) via supervised fine-tuning. We henceforth denote it as the SFT model.

106 ²Regarding a detailed comparison of the differences between the two abilities, please refer to Appendix B.

107 ³VQA datasets include GQA (Hudson & Manning, 2019), TextVQA (Singh et al., 2019), and MME (Fu
 108 et al., 2024), and CR datasets include SugarCrepe (Hsieh et al., 2023), SADE (Ma et al., 2023), BiVLC (Mi-
 109 randa et al., 2024), and Winoground (Thrush et al., 2022). Results in Figure 1(a) correspond to the average
 110 performance across the datasets.

We summarize our contributions as follows: (1) We identify, for the first time, that existing KD methods in MLLMs fail to distill visual perception ability from the teacher and provide a detailed attention-based analysis, offering insights on how to enhance this ability. (2) We propose **CompoDistill**, a novel KD framework that transfers both visual recognition and perception abilities through the Visual ATtention alignment and the Teacher Adapter Fetch Module. (3) We achieve significant improvements in CR tasks by effectively distilling the visual perception ability, while maintaining competitive performance in VQA tasks by preserving the visual recognition ability.

2 PRELIMINARY

Multimodal Large Language Models (MLLMs). Following the LLaVA (Liu et al., 2023) design, MLLMs consist of three main components: a pre-trained LLM $LM_\theta(\cdot)$, a vision encoder $V_\phi(\cdot)$, and an adapter $P_\psi(\cdot)$. Given a text query Q and an image $I \in \mathbb{R}^{H \times W \times 3}$, where H and W denote the image height and width, the vision encoder extracts patch-level features $\mathbf{z}_p = V_\phi(I) \in \mathbb{R}^{N_v \times d_p}$, with N_v being the number of visual patches and d_p the hidden dimension of V_ϕ . The adapter projects them into the language space as $\mathbf{x}_v = P_\psi(\mathbf{z}_p) \in \mathbb{R}^{N_v \times d}$, where d is the hidden dimension of LM_θ . Hereafter, we refer to \mathbf{x}_v as the *visual tokens*. Meanwhile, the query Q is tokenized into embeddings $\mathbf{x}_t \in \mathbb{R}^{N_t \times d}$, where N_t is the number of text tokens. The combined sequence $[\mathbf{x}_v, \mathbf{x}_t] \in \mathbb{R}^{(N_v + N_t) \times d}$ is processed by the LM_θ to compute the probability of the target answer as:

$$p(\mathbf{y}_{1:K}) = \prod_{i=1}^K p(\mathbf{y}_i \mid \mathbf{x}_v, \mathbf{x}_t, \mathbf{y}_{<i}), \quad (1)$$

where $\mathbf{y}_{<i}$ is the sequence of the answer tokens up to the i -th token and K is the answer length. During training, the cross-entropy loss derived from Equation 1 is minimized, denoted as \mathcal{L}_{LM} .

3 WHY IS THE VISUAL PERCEPTION ABILITY NOT DISTILLED PROPERLY?

In Section 1, we noted that existing KD methods, despite improvements in terms of VQA, show unexpected results on compositional reasoning (CR) tasks, which we attribute to **visual attention misalignment**. This section provides an in-depth analysis to elucidate the underlying causes of this issue. Our analysis first identifies the key factor for distilling visual ability through an attention-based analysis (Section 3.1), then demonstrates this factor’s direct impact on performance (Section 3.2). Finally, we validate that alleviating the visual attention misalignment associated with this key factor facilitates a more effective transfer of visual perception (Section 3.3).

3.1 IDENTIFYING THE KEY FACTOR: TEACHER-STUDENT ATTENTION SIMILARITY OVER VISUAL TOKENS IN THE VISUAL UNDERSTANDING LAYER

In this section, we aim to identify a critical factor that can serve as a criterion for successfully distilling visual abilities (i.e., visual recognition and perception). To achieve this, we examine the layer-wise functions of the LLM within MLLMs, building on insights from prior works (Chen et al., 2025a; Yoon et al., 2025). This is followed by an attention-based analysis to pinpoint the key factor.

Layer-wise Functionality in MLLMs. Following previous studies (Chen et al., 2025a; Yoon et al., 2025), we adopt a layer-wise view of MLLM processing: *Early layers* align heterogeneous modalities with the LLM’s text space, *Intermediate layers* integrate these signals for fine-grained semantic understanding, and *Later layers* generate the final response. Our focus is on the intermediate layers⁴, which we term the **visual understanding layers**, since these layers play a critical role in forming foundational visual reasoning and comprehension (Chen et al., 2025b), which are closely tied to the visual abilities (recognition and perception) central to our study.

Attention Analysis for VQA and CR Tasks. Building on our focus on the visual understanding layers, we design an experiment to investigate if teacher-student attention alignment can explain the difference in the degree of performance improvement between VQA and CR tasks, as observed in Figure 1(a). To this end, we compare the attention distribution of the teacher model (i.e., LLaVA-4B (Liu et al., 2023) with that of two distinct models: a student model distilled directly from the teacher (i.e., LLaVA-KD-2B (Cai et al., 2024)) and an SFT model (i.e., LLaVA-2B) that is architecturally identical to the student model but trained without distillation.

As shown in Figure 2(a), we measure the attention similarity to quantify the alignment between a given model (student or SFT) and the teacher. This is computed as the cosine similarity of

⁴Following (Neo et al., 2025), intermediate layers refer to the 30–70% range of the total LLM layers.

162 their attention distributions, where the answer token y_i is the *query* (Q) and the **visual tokens**
 163 (x_v) or **text tokens** (x_t) are the *key* (K). Our primary analysis centers on the attention distributions
 164 over **visual tokens** during answer generation, as these are critical for the visual abilities being
 165 studied. For a more comprehensive comparison, we also investigate attention distribution over
 166 **text tokens**. We analyze the attention similarity of the student and SFT models to the teacher.
 167 Specifically, we investigate how these similarities in attention behavior are related with each model’s performance
 168 in VQA and CR task, which brings us closer to identifying the key factor. To guide this investigation, we formulate
 169 two key research questions:
 170

Q1) Where do the performance gains of KD on VQA (visual recognition) tasks originate? For **VQA**, where the student model demonstrates clear performance improvements, Figure 2(b) shows that, within the **visual understanding layers**, the teacher-student attention similarity over **visual tokens** is significantly higher than that between the teacher-SFT. However, no such improvement is observed for **text tokens** (Figure 2(d)). This finding brings us to identify the clue of the key factor: *if the teacher-student visual attention similarity in the visual understanding layers is high, distillation is effectively achieved, resulting in performance improvement of the student* .

Q2) Why does KD fail to deliver comparable improvements on CR (visual perception) tasks? We extend our analysis to **CR** tasks, where the student model performs on par with the SFT model. As shown in Figure 2(c) and (e), we observe that the teacher-student attention similarity is comparable to the teacher-SFT attention similarity in the **visual understanding layers**, even over the **visual tokens**, which contrasts with our observation on VQA. That is, in the **visual understanding layers**, the student model shows no better alignment with the teacher model in terms of the attention over **visual tokens** than the SFT model, despite such alignment being crucial for success in the downstream performance as shown in the case of VQA. Drawing on the findings from **Q1** and **Q2**, we argue that the inability of existing KD methods to effectively distill visual perception ability stems from the moderate level of teacher-student attention similarity in the **visual understanding layers**.

3.2 RELATIONSHIP BETWEEN TEACHER-STUDENT ATTENTION SIMILARITY AND DOWNSTREAM PERFORMANCE

While the teacher-student attention similarity over **visual tokens** appears to be a key factor in determining whether visual abilities have been distilled, its direct relationship with downstream performance remains unclear. In other words, it is uncertain whether the higher teacher-student attention similarity (green line), relative to the teacher-SFT attention similarity (yellow line) in the visual understanding layers (Figure 2(b)), explains the superior performance of the student model on the VQA dataset. To this end, we quantify the relationship between the teacher-student **visual attention similarity** and the **answer token probability** given in Equation 1 on the VQA dataset (Figure 3), where visual recognition ability has been successfully distilled from the teacher model. More precisely, we randomly sampled 5,000 instances from the GQA test set, grouped them according to the student-teacher similarity over visual tokens during the answer generation step, and then measured the average probability assigned to the ground-truth answers. The results reveal a clear positive trend: higher attention similarity is consistently associated with higher answer probabilities, providing direct evidence that aligning the student’s attention with the teacher’s attention is a key factor driving better performance on VQA.

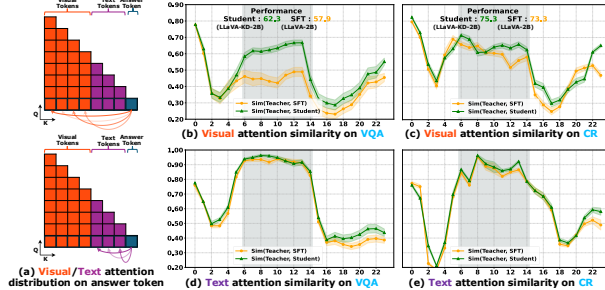


Figure 2: (a) Attention of the answer token over **visual tokens** and **text tokens** during its generation. The transparency indicates the degree of attention the answer token gives to these tokens. (b-e) Layer-wise Teacher-Student and Teacher-SFT attention similarities over **visual tokens** ((b), (c)) and **text tokens** ((d), (e)). GQA is used for **VQA** ((b), (d)), and SugarCrepe is used for **CR** ((c), (e)). Results on other datasets are shown in Appendix C.

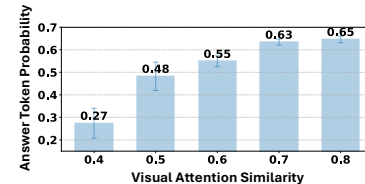


Figure 3: Relationship between attention similarity and performance on the GQA (VQA) dataset.

3.3 A SIMPLE SOLUTION: REPLACING STUDENT’S VISUAL ATTENTION WITH TEACHER’S

216 **Is Teacher Attention Really Beneficial?** A natural question arises: *Does increasing the teacher-student attention*
 217 *similarity over visual tokens —a key factor for VQA performance—also enhance performance on CR tasks?* To test
 218 this, we perform a direct intervention during inference on
 219 CR. Before generating the answer, we substitute the student’s original attention over visual tokens with the average
 220 of the teacher’s and student’s attention, thereby increasing the student’s attention similarity to the teacher⁵. (Figure 4). This
 221 yields modest but consistent performance gains in the Sugar-
 222 Crepe dataset (Swap, Replace and Add are three types of CR sub-tasks in the dataset). Although
 223 small, these improvements confirm that the student benefits from incorporating the teacher’s attention,
 224 reinforcing our hypothesis that attention alignment plays a crucial role in effective knowledge
 225 transfer.
 226

227 In summary, our analysis identifies *visual attention misalignment* as the key barrier to effectively
 228 distilling the teacher’s perception abilities to the student, highlighting the crucial need to accurately
 229 transfer the teacher’s visual attention.

4 METHODOLOGY: COMPODISTILL

230 Motivated by the findings in Section 3, our framework, called CompoDistill, is designed to effec-
 231 tively transfer the teacher’s visual perception abilities by addressing the visual attention misalign-
 232 ment. We first introduce our two core components: the **Visual ATtention alignment (VAT)** module
 233 (Section 4.1), which aligns the student’s visual attention mechanism with that of the teacher, and the
 234 **Teacher Adapter Fetch (TAF)** module (Section 4.2), which ensures the student processes visual
 235 space consistently with the teacher. These modules are then integrated into a meticulously designed
 236 three-stage training strategy (Section 4.3). The overall framework is shown in Figure 5.

4.1 VISUAL ATTENTION ALIGNMENT (VAT) MODULE

237 **Attention Distillation Loss.** To transfer the teacher’s attention mechanism to the student, we util-
 238 ize the attention matrix of the Transformer (Vaswani et al., 2017) within the LLM layer, which
 239 represents the importance of each token relative to other tokens. The attention matrix for the input
 240 tokens (i.e., \mathbf{x}_v and \mathbf{x}_t) is computed as: $A = \text{softmax}(\mathbf{Q}\mathbf{K}^\top/\sqrt{d}) \in \mathbb{R}^{(N_v+N_t) \times (N_v+N_t)}$, where
 241 $\mathbf{Q} \in \mathbb{R}^{(N_v+N_t) \times d}$ and $\mathbf{K} \in \mathbb{R}^{(N_v+N_t) \times d}$ are the query and key matrices derived from the input
 242 tokens, respectively. From the overall attention matrix A , as discussed in Section 3, our goal is to
 243 distill the *attention over visual tokens* from the teacher to the student in the visual understanding
 244 layers, leading us to extract a sub-matrix $\tilde{A} \in A$ that focuses on visual attention. Specifically, for each
 245 visual understanding layer l , this sub-matrix includes only the columns (keys) of A_l corresponding
 246 to the visual tokens, resulting in $\tilde{A}_l = A_l[:, :N_v] \in \mathbb{R}^{(N_v+N_t) \times N_v}$. Based on the visual attention-
 247 related sub-matrices of the teacher (\tilde{A}_l^t) and student (\tilde{A}_l^s), we compute the cosine distance between
 248 them for the attention distillation loss as $1 - \text{sim}(\tilde{A}_{l_t}^t, \tilde{A}_{l_s}^s)$, where l_t and l_s denote the index of the
 249 visual understanding layers of the teacher and student, respectively.

250 **Group Layer Matching.** However, since the teacher has more layers than the student, directly
 251 matching a student layer index l_s with a teacher layer index l_t is challenging. A naive solution
 252 is to map each l_s to one l_t by uniformly sampling teacher layers according to the ratio of their
 253 depths. For example, if the student has 5 layers and the teacher has 10 layers, then teacher layers
 254 $\{1, 3, 5, 7, 9\}$ are selected and aligned with the 5 student layers. However, this approach is subop-
 255 timal, as it overlooks the richer perception abilities distributed across the teacher’s layers and does
 256 not ensure accurate alignment⁶. Instead, we propose a simple yet effective **Group Layer Matching**
 257 strategy, where each l_s is aligned with a group of $\{l_t\}$ in a one-to-many manner, enabling the student
 258 to capture broader teacher knowledge while roughly preserving the layer order.

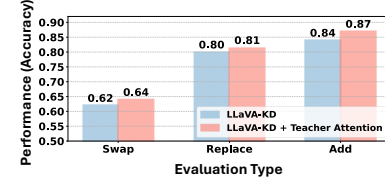


Figure 4: Change in performance the student attention is substituted with the teacher attention on the SugarCrepe (CR) dataset.

⁵We initially attempted to completely replace the student’s attention with that of the teacher. However, this rather led to a slight performance degradation compared with vanilla LLaVA-KD, which we attribute to a mismatch between the student’s feature space and the teacher’s attention.

⁶In Table 3, we show that this approach is less effective than the proposed Group Layer Matching strategy.

270 Formally, let the sequence of student’s visual understanding layer indices be $L_S = \{l_s^1, \dots, l_s^j, \dots, l_s^k\}$ and that of the teacher be $L_T = \{l_t^1, \dots, l_t^j, \dots, l_t^m\}$, where j is the j -th layer in the visual 271 understanding layers, and k and m denote the total number of visual understanding layers for the 272 student and teacher, respectively, with $k < m$. For each student layer l_s^j , we define a corresponding 273 group of teacher layers, G_j , consisting of n^7 consecutive teacher layers, formed using a sliding 274 window approach. For example, the group of teachers G_1 assigned for the first student layer l_s^1 could 275 be $\{l_t^1, l_t^2, \dots, l_t^n\}$, while the group G_2 for the second student layer l_s^2 would be $\{l_t^2, l_t^3, \dots, l_t^{n+1}\}$, 276 and so on. So, the total number of groups is the same as the number of student’s target layers, k . 277

278 To distill the visual attention of a teacher group G_j into student layer l_s^j , we formulate the objective by minimizing the 279 cosine distance between the attention matrix of student layer, $\tilde{A}_{l_s^j}^s$, and the averaged attention 280 matrices of its corresponding teacher group, \bar{A}_j^t , as follows: 281

$$284 \mathcal{L}_{ADL} = 1 - \frac{1}{k} \sum_{j=1}^k \text{sim}\left(\bar{A}_j^t, \tilde{A}_{l_s^j}^s\right), \bar{A}_j^t = \frac{1}{n} \sum_{l \in G_j} \tilde{A}_l^t. \quad (2)$$

285 Furthermore, beyond the naive one-to-one matching approach, 286 our proposed group matching strategy is superior to the more 287 advanced adaptive matching method (Lee et al., 2025b) in terms 288 of effectiveness, as demonstrated in Section 5.3. 289

291 4.2 TEACHER ADAPTER FETCH (TAF) MODULE

292 The adapter, responsible for projecting the visual space into the 293 language space of the LLM, is crucial for generating the visual 294 tokens with which the attention mechanism processes. In this 295 regard, given that the teacher’s attention mechanism transferred 296 via VAT is tightly coupled with the output of its own adapter, 297 a vision-language space mismatch occurs when this attention is 298 imposed on a student with a different, incompatible space, hindering 299 effective knowledge transfer. To address this, we introduce the 300 **Teacher Adapter Fetch (TAF)** module, which directly 301 leverages the teacher’s frozen, pretrained adapter ($P_{\psi_t}^t$) and adds 302 a lightweight trainable MLP ($P_{\psi_s}^s$) only for dimensional alignment. 303 This ensures the student processes the visual input through 304 the same lens as the teacher, making the attention transfer effective. 305 Formally, the student’s visual token is expressed as follows:

$$306 \mathbf{x}_v = P_{\psi_s}^s \left(P_{\psi_t}^t (\mathbf{z}_p) \right) \in \mathbb{R}^{N_v \times d_s}, \quad (3)$$

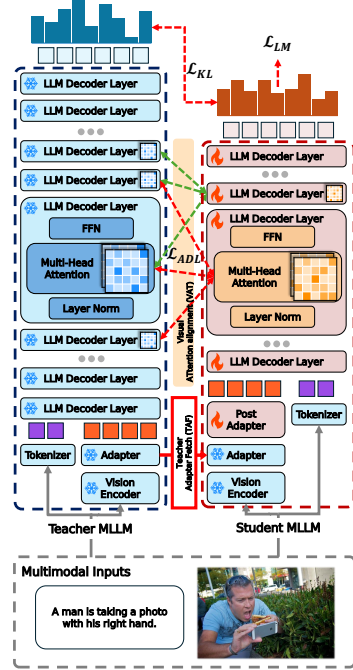
307 where d_s is the hidden dimension of the student LLM. This approach allows for the student to bridge 308 the gap between the teacher-imposed attention mechanism and its own visual feature space. 309

310 **Discussion.** It is important to note that attention distillation itself is not a novel concept, as similar 311 approaches have been explored in various domains (Wang et al., 2020; Sajedi et al., 2023; Zhou 312 et al., 2025), including diffusion models, dataset distillation, and language models. However, its 313 application to MLLMs is particularly challenging due to mismatched visual feature spaces between 314 teacher and student. To this end, we introduce the TAF module as a simple yet effective solution 315 that makes attention distillation practical in this setting. Lastly, our work is not intended to propose 316 a fundamentally new distillation method; rather, its primary contribution lies in identifying a critical 317 factor that can serve as a criterion for successfully distilling visual abilities in MLLMs, i.e., visual 318 attention misalignment, as explained in Section 3.

319 4.3 THREE-STAGE DISTILLATION FRAMEWORK

320 Our knowledge distillation framework consists of three stages, built upon two foundational training 321 objectives. The first objective is language modeling autoregressive loss \mathcal{L}_{LM} , as defined in 322 Section 2. Moreover, following previous studies (Shu et al., 2024; Cai et al., 2024), we employ 323

⁷To ensure the use of all teacher layers L_T , we define n in closed form as $m - k + 1$.



324 Figure 5: Overview of CompoDistill. It consists of the VAT module and the TAF module.

324 a Kullback-Leibler (KL) divergence loss (\mathcal{L}_{KL}) to align the student’s predictive distribution (p_s)
 325 with the teacher’s (p_t), encouraging the student to mimic the teacher’s final output at the logit level:
 326

$$327 \quad \mathcal{L}_{KL} = -\frac{1}{K} \sum_{k=1}^K \sum_{n=1}^N p_t(\mathbf{y}_n | \mathbf{x}_v, \mathbf{x}_t, \mathbf{y}_{<k}) \log \frac{p_t(\mathbf{y}_n | \mathbf{x}_v, \mathbf{x}_t, \mathbf{y}_{<k})}{p_s(\mathbf{y}_n | \mathbf{x}_v, \mathbf{x}_t, \mathbf{y}_{<k})}, \quad (4)$$

328 where \mathbf{y}_n is the n -th vocabulary token and N is the total vocabulary size.
 329

330 **Stage 1: Distilled Pre-Training (DPT).** The first stage aims to align the visual feature space with
 331 the language space. To this end, instead of initializing an adapter from scratch, we construct it using
 332 our **Teacher Adapter Fetch** module, which reuses the teacher’s pretrained adapter, which is kept
 333 frozen during training. While the vision encoder and LLM remain frozen, the student adapter $P_{\psi_s}^s$ is
 334 optimized with the language modeling loss (\mathcal{L}_{LM}) and the KL-divergence loss (\mathcal{L}_{KL}).
 335

336 **Stage 2: Distilled Fine-Tuning (DFT).** In the second stage, we aim to enhance the student’s visual
 337 perception by aligning its visual attention mechanism over visual tokens with that of the teacher via
 338 the **Visual ATtention Alignment** module. During this stage, both the student LLM and the student
 339 adapter $P_{\psi_s}^s$ are fine-tuned. The overall objective is defined as $\mathcal{L}_{LM} + \mathcal{L}_{KL} + \mathcal{L}_{ADL}$.
 340

341 **Stage 3: Supervised Fine-Tuning (SFT).** Finally, motivated by prior work (Lee et al., 2025b), we
 342 fine-tune only the student using the autoregressive language modeling loss (\mathcal{L}_{LM}), with both the
 343 student LLM and the student adapter $P_{\psi_s}^s$ trained in the same manner as in Stage 2. This final stage
 344 consolidates the rich knowledge transferred from the teacher during Stages 1 and 2 into the student’s
 345 own parameters and further strengthens its instruction-following capability.
 346

347 5 EXPERIMENTS

348 5.1 EXPERIMENTAL SETTINGS.

349 **Evaluation Benchmarks.** For evaluation, we use two categories of vision-language tasks. **General**
 350 **VQA**: We evaluate visual recognition abilities using well-established benchmarks including
 351 VQAv2 (Goyal et al., 2017), GQA (Hudson & Manning, 2019), and VizWiz (Bigham et al., 2010)
 352 for question answering, TextVQA (Singh et al., 2019) for scene text comprehension, and MME (Fu
 353 et al., 2024) for comprehensive multimodal evaluation. **Compositional Reasoning**: To evaluate vi-
 354 sual perception abilities, we use several challenging benchmarks: SugarCrepe (Hsieh et al., 2023),
 355 SADE (Ma et al., 2023), BiVLC (Miranda et al., 2024), and Winoground (Thrush et al., 2022). We
 356 use accuracy as the evaluation metric. Refer to Appendix D for more details regarding the baselines.
 357

358 **Implementation Details.** Both the student and teacher employ SigLIP (Zhai et al., 2023) vision en-
 359 coder and the Qwen 1.5 (Yang et al., 2024) LLM series, with the student having 1.8B parameters and
 360 the teacher having 4B parameters. Regarding the details of the training datasets and hyperparameter
 361 settings, please refer to Appendix E.
 362

363 5.2 QUANTITATIVE RESULTS ON VQA AND CR TASKS

364 In Table 1, we compare CompoDistill with a diverse range of MLLMs of different sizes on VQA
 365 and CR tasks, which evaluate visual recognition and perception abilities, respectively. We have the
 366 following key observations: **1)** Existing KD methods⁸ outperform the SFT model (LLaVA-2B) on
 367 VQA (visual recognition) tasks, but not on CR (visual perception) tasks, where their performance
 368 remains comparable to that of standard 2B models. This indicates that KD methods struggle to dis-
 369 till visual perceptual abilities. **2)** CompoDistill overcomes this limitation by significantly improving
 370 CR performance to a level competitive with 4B models—an achievement not attained by previ-
 371 ous KD methods—while simultaneously maintaining strong, state-of-the-art performance on VQA.
 372 This demonstrates the ability of CompoDistill to enhance visual perception while maintaining vi-
 373 sual recognition. **3)** CompoDistill achieves these results with high data efficiency, relying on just
 374 1.2M training samples. This is a sharp contrast to other models requiring much larger datasets (e.g.,
 375 LLaVA-MoD with 5M, MiniCPM-V with 570M), proving the effectiveness of CompoDistill toward
 376 a truly efficient MLLM.
 377

378 5.3 ABLATION STUDIES

379 **Effect of Core Components.** In Table 2, we conduct ablation studies to understand the effect of
 380 each component (i.e., VAT and TAF modules). Note that the variant without either component (row
 381

382 ⁸To ensure fair comparisons, all KD models were distilled from the same teacher model (i.e., LLaVA-4B)
 383 and share the same LLM backbone (i.e., Qwen 1.5).
 384

378 Table 1: Comparison **CompoDistill** with KD-based methods and other MLLMs on VQA and CR. # Samples :
379 Training data samples. [†]:Reproduced results using the official source code. The best and second-best models
380 are marked in bold and underlined, respectively for models sizes under 2B.

Size	Method	LLM	# Samples	Visual Question Answering						Compositional Reasoning				
					VQA v2	VizWiz	GQA	TextVQA	MME	Avg		Sugarcreep	SADE	BiVLC
~7B	LLaVA-7B [†]	Qwen1.5-7B	1.2 M	79.8	53.1	62.3	60.1	68.6	64.8	87.3	78.5	65.7	58.4	72.5
	LLaVA-7B [†]	Qwen2.5-7B	1.2 M	81.4	50.6	63.8	64.6	77.5	67.6	93.1	82.9	68.3	68.2	78.1
	CogVLM-7B	Vicuna-7B	1500 M	82.3	-	64.9	78.2	71.8	-	81.8	63.2	64.5	57.2	66.7
	Qwen2.5-VL-7B	Qwen2-7B	1500 M	82.8	61.7	63.9	73.9	83.9	73.2	88.5	77.4	68.4	75.3	77.4
	Deepseek-VL-7B	DLLM-7B	2000 M	-	49.9	61.3	64.7	73.4	-	86.2	78.8	66.2	61.7	73.2
~4B	LLaVA-4B [†] (Teacher)	Qwen1.5-4B	1.2 M	79.1	48.0	62.1	56.7	67.2	62.6	83.0	75.5	64.8	57.8	70.3
	Qwen2.5-VL-3B	Qwen2-3B	1.2 M	80.4	54.1	60.9	68.5	72.8	67.3	97.1	65.9	67.0	63.5	63.4
	Imp-3B	Phi2-2.7B	1.5 M	81.2	54.1	63.5	59.8	72.3	66.2	78.1	61.1	59.5	38.3	59.3
	Bunny-3B	Phi2-2.7B	2.6 M	79.8	43.8	62.5	56.7	74.4	63.4	75.8	67.2	59.7	53.1	64.0
	MoE-LLaVA-3B	Phi2-2.7B	2.6 M	79.9	43.7	62.6	57.0	71.6	63.0	80.5	70.4	64.4	54.1	67.3
~2B	MobileVLM-3B	MobileLLaMA-2.7B	1.3 M	-	-	61.1	57.5	72.0	-	67.9	72.1	57.2	43.9	60.3
	MiniCPM-V	MiniCPM-2.4B	570 M	-	60.2	52.1	73.2	70.5	-	90.0	70.6	65.3	55.3	70.3
	MiniGemini-2B	Gemma-2B	2.7 M	-	41.5	60.7	56.2	67.0	-	67.0	62.0	58.0	50.5	59.4
	Deepseek-VL-1.3B	DLLM-1.3B	2000 M	-	36.8	59.3	58.4	65.3	-	36.6	38.6	39.9	60.8	44.0
	MobileVLM-1.7B	MobileLLaMA-1.4B	1.2 M	-	-	59.3	52.1	65.1	-	69.8	64.0	53.8	43.4	57.7
~1B	Imp-2B	Qwen1.5-1.8B	1.5 M	79.2	39.2	61.9	54.5	65.2	60.0	71.0	59.6	58.5	51.1	60.1
	Bunny-2B	Qwen1.5-1.8B	2.6 M	76.6	34.2	59.6	53.2	65.0	57.7	68.6	66.5	57.8	48.5	60.3
	MoE-LLaVA-2B	Qwen1.5-1.8B	2.2 M	76.2	32.6	61.5	48.0	64.6	56.6	80.8	62.5	62.0	50.6	63.9
	LLaVA-2B (SFT model)	Qwen1.5-1.8B	1.2 M	73.6	31.2	57.9	50.6	61.2	54.9	73.3	63.9	58.5	47.2	60.7
	LLaVA-KD-2B	Qwen1.5-1.8B	1.2 M	78.8	44.8	62.3	53.4	68.9	61.6	75.3	63.6	57.9	49.3	61.5
~0.5B	LLaVA-VAD-2B [†]	Qwen1.5-1.8B	1.2 M	75.8	35.2	58.7	49.4	63.8	56.6	76.9	61.5	54.1	48.4	60.2
	LLaVA-MoD-2B [†]	Qwen1.5-1.8B	5.0 M	76.3	43.0	58.8	52.7	63.4	58.9	76.9	63.8	60.3	49.4	62.6
	CompoDistill-2B	Qwen1.5-1.8B	1.2 M	78.8	42.5	62.2	56.4	70.1	61.9	82.9	69.4	63.3	51.2	66.7

396 Table 2: Ablation for VAT and TAF modules.

Row	VAT module	TAF module	Visual Question Answering				Compositional Reasoning					
				GQA	TextVQA	MME	Avg		Sugarcreep	SADE	BiVLC	Winoground
(a)	✗	✗		57.8	50.1	62.5	56.8		76.3	64.9	61.7	48.7
(b)	✓	✗		54.3	54.6	64.8	57.9		81.0	66.4	62.1	50.5
(c)	✗	✓		60.8	56.5	66.5	61.3		78.0	67.0	62.4	48.1
(d)	✓	✓		62.2	56.4	70.1	62.9		82.9	69.4	63.3	51.1
												66.7

403 (a)) follows the proposed three-stage framework (Section 4.3), using only the language modeling
404 loss (Section 2) and logit-based KD loss (Equation 4). **Effect of VAT module**: We observe that the
405 VAT module significantly improves the performance especially on CR tasks (row (a) vs. (b) and row
406 (c) vs. (d)), demonstrating the effectiveness of enhancing visual perception abilities. This confirms
407 that explicit visual attention alignment is crucial for distilling visual perception ability, as discussed
408 in Section 3. **Effect of TAF module**: We observe that equipping the TAF module improves the
409 performance on VQA and CR tasks (row (a) vs. (c) and row (b) vs. (d)), indicating that bridging
410 the student’s feature space with the imposed attention mechanism is crucial for effective knowledge
411 transfer. Finally, the fully-fledged model (row (d)) achieves the best performance on both VQA and
412 CR tasks, demonstrating the benefit of the VAT and TAF modules.

413 Table 3: Detailed ablation for VAT module. The blue line performs the same as CompoDistill.

414 (a) Attention loss type (b) Target layers (c) Layer matching strategy

Attention Loss	VQA Avg	CR Avg	Target Layers	VQA Avg	CR Avg	Match strategy	VQA Avg	CR Avg
✗	61.3	63.8	Early (~30%)	61.2	63.7	Simple	61.5	65.6
MSE	60.3	65.2	Later (70% ~)	61.7	64.6	Adaptive	62.0	65.7
KL. Div.	60.7	65.5	All	62.4	66.6	Group	62.9	66.7
Cos. Sim.	62.9	66.7	Intermediate	62.9	66.7			

420 **Fine-grained Analysis on VAT module.** We perform fine-grained ablation studies to study the impact
421 of specific design choices—namely, the attention loss type, the target matching layer, and the
422 layer matching strategy—within the VAT module. **1)** We first analyze the impact of the **attention**
423 **loss function** (Table 3a). While any form of attention loss improves CR over the baseline, using
424 Cosine Similarity (Cos. Sim.) significantly outperforms both MSE and KL Divergence. This result
425 suggests that it is more crucial for the student to learn the relative importance among visual patches
426 rather than forcing an exact match of their absolute attention scores. **2)** Next, we investigate **which**
427 **layers to target for distillation** (Table 3b). Performing distillation on the intermediate layers (30-
428 70%) yields the highest performance. This finding confirms our analysis that *visual understanding*
429 layers are crucial for visual-semantic integration and highlights the effectiveness of distilling specifically
430 from these layers, a strategy consistent with prior research (Kaduri et al., 2024). **3)** Lastly, we
431 evaluate different **layer matching strategies** (Table 3c). Our proposed Group matching achieves the
432 best performance compared to both Simple matching (which uniformly samples teacher layers) and
433 Adaptive matching (which finds optimal pairs based on layer distance). This suggests that grouping

432 layers provides a more stable and effective signal for transferring the teacher’s complex attention
 433 behaviors, especially when student and teacher architectures differ in depth.⁹
 434

435 **Further Benefit on Other Complex Task.** Beyond compositional reasoning, we explore a further benefit of enhancing
 436 visual perception for complex tasks. Specifically, we expect
 437 that CompoDistill can help mitigate the relational hallucinations,
 438 thanks to its ability to accurately understand object
 439 relationships, as discussed in Section 1. To test this, we evaluate
 440 CompoDistill on the R-Bench (Wu et al., 2024) and Reef-
 441 knot (Zheng et al., 2025) benchmarks, both of which focus on evaluating relational hallucinations.
 442 As shown in Table 4, CompoDistill significantly outperforms other KD methods and achieves per-
 443 formance nearly on par with the teacher. The results highlight that enhancing the visual perception
 444 ability can be beneficial to not only compositional reasoning tasks but also other complex tasks that
 445 require precise understanding of relationships among objects.

6 SCALABILITY EXPERIMENTS

446 **Richer Data Improves Distillation Performance.** We ana-
 447 lyze the effect of data scale in Table 5. Performance improves
 448 significantly when moving from SFT to distillation, and in-
 449 creases further when the training dataset size is doubled¹⁰. This
 450 highlights that both the quality and quantity of training data are
 451 crucial for effective knowledge transfer, with CR showing particular sensitivity to data scaling.

452 **Larger Teachers Produce Stronger Students.** Next, we exam-
 453 ine the influence of teacher model size in Table 6. Our experi-
 454 ments show that students consistently benefit from larger teach-
 455 ers, regardless of the student’s own size. For instance, a 1.8B
 456 student distilled from a 7B teacher outperforms one distilled
 457 from a 4B teacher. This demonstrates that a higher-capacity
 458 teacher is crucial for transferring stronger reasoning abilities,
 459 providing a more effective source of knowledge for the student.

460 **Our Distillation Method Generalizes Across Backbones.** Finally, we test our framework’s generalizability by replac-
 461 ing the Qwen backbone with the MobileLLaMA family (ML-
 462 LaMA) in Table 7. Our distillation method remains effec-
 463 tive even with this entirely different architecture. This result
 464 confirms the robustness and generalizability of our approach,
 465 demonstrating that its principles are not tied to a specific model family but are broadly applicable.

7 RELATED WORKS

466 **Multimodal Large Language Models.** Visual instruction tuning (Liu et al., 2023) has propelled
 467 MLLMs to strong performance on diverse benchmarks (Chen et al., 2024; Yang et al., 2024; OpenAI,
 468 2023), yet persistent weaknesses remain in fine-grained visual tasks (Tong et al., 2024; Qi et al.,
 469 2025). Early efforts to address these limitations focused on scaling up vision encoders (Lu et al.,
 470 2024; Kar et al., 2024) or designing more expressive projectors (Cha et al., 2024; Liu et al., 2024).
 471 More recently, the focus has shifted to the internal information flow, with research identifying critical
 472 failures such as misaligned attention (Jiang et al., 2025; Neo et al., 2025; Dariset et al., 2024) and
 473 the dilution of visual features in intermediate layers (Kaduri et al., 2024; Yoon et al., 2025; Chen
 474 et al., 2025b). In contrast to these approaches, our analysis focuses on the visual attention dynamics
 475 between student and teacher models trained via direct knowledge distillation.

476 **Knowledge Distillation.** Knowledge distillation (KD) compresses a large teacher model into a
 477 smaller, efficient student (Hinton et al., 2015), a technique widely applied to LLMs via logit match-
 478 ing (Sun et al., 2019; Jiao et al., 2020). In the multimodal domain, methods have adapted this for
 479 visual grounding (Cai et al., 2024; Feng et al., 2025) or used modular strategies to overcome architec-
 480

Table 4: Comparison for relational hallucination using F1 score.

Model	R-Bench ↑	Reefknot ↑
Teacher (LLaVA-4B)	79.1	67.9
Student (LLaVA-2B)	74.3	61.3
LLaVA-KD-2B	76.5	60.3
LLaVA-Mod-2B	76.2	63.4
CompoDistill-2B	78.6	66.7

Table 5: Data Scaling Experiment.

Student	# Sample	VQA Avg	CR Avg
Qwen1.5-1.8B (SFT)	1.2 M	56.6	60.7
Qwen1.5-1.8B	1.2 M	62.9	66.7
Qwen1.5-1.8B	2.4 M	63.3	69.9

Table 6: Experiments with different size of teacher/student.

Student	Teacher	VQA Avg	CR Avg
Qwen1.5-1.8B (SFT)		56.6	60.7
Qwen1.5-1.8B	Qwen1.5-4B	62.9	66.7
Qwen1.5-1.8B	Qwen2.5-7B	63.4	67.8
Qwen1.5-0.5B (SFT)		52.0	48.4
Qwen1.5-0.5B	Qwen1.5-1.8B	54.7	51.1
Qwen1.5-0.5B	Qwen1.5-4B	56.6	54.5

Table 7: Experiments with a different LLM backbone.

Student	Teacher	VQA Avg	CR Avg
MLLaMA-1.7B (SFT)		49.7	43.7
MLLaMA-1.7B	MLLaMA-3B	53.1	48.9

⁹For a detailed explanation of the layer matching strategies, see Appendix F.

¹⁰For details on the training data, see Appendix G.

tural limits (Shu et al., 2024). The scope has since expanded to distillation across model families (Lee et al., 2025b;a) and a deeper focus on internal mechanics. For instance, recent alignment-oriented methods like VIRAL (Yoon et al., 2025) regularize intermediate representations to preserve visual semantics, moving beyond simple logit-level supervision. While these studies primarily propose new distillation techniques, our work takes a different approach. We instead provide a detailed analysis to identify the specific bottlenecks that hinder the effectiveness of knowledge distillation in MLLMs.

Compositional Reasoning Benchmarks. Compositional reasoning, the ability to understand the interplay of objects and their relations, remains a significant hurdle for vision–language models. Initial benchmarks like Winoground (Thrush et al., 2022) first exposed these weaknesses in early models. Building on this, a new generation of more robust benchmarks has emerged to address evaluation biases. These include SugarCrepe (Hsieh et al., 2023), which uses LLM-generated hard negatives; SADE (Ma et al., 2023), which specifically diagnoses and mitigates the language bias found in generative models through a debiased test set that neutralizes syntactic shortcuts; and BiVLC (Miranda et al., 2024), which focuses on bidirectional retrieval with synthetic negatives.

8 CONCLUSION

In this work, we aim to enhance the visual perception abilities of Knowledge Distillation(KD)-based Multimodal Large Language Models (MLLMs), which has been largely overlooked by the previous KD studies. To this end, we conduct a systematic analysis and identify visual attention misalignment as a key factor hindering the effective distillation of visual perception from teacher to student. Building on this analysis, we propose CompoDistill, a novel KD framework that incorporates a Visual ATtention alignment (VAT) module to explicitly address this misalignment. Furthermore, we introduce the Teacher Adapter Fetch (TAF) module to ensure that teacher-imposed attention mechanism is compatible with the student’s feature space, making synergy with VAT module. Through extensive experiments on VQA and CR benchmarks, we demonstrate that CompoDistill significantly enhances visual perception abilities while preserving strong visual recognition abilities, as achieved in existing KD works. Regarding the limitation and future work, please refer to Appendix P.

We believe that this work provides a novel perspective on the student’s visual attention misalignment and makes a contribution to the pursuit of efficient MLLMs, especially in KD-based research, by establishing the first dedicated direction toward enhancing visual perception abilities.

ETHICS STATEMENT

Our research contributes to the development of more efficient and accessible Multimodal Large Language Models (MLLMs). By enabling the creation of smaller, yet highly capable student models, our work helps lower the significant computational barriers to deploying advanced AI, promoting its broader adoption. In compliance with the ICLR Code of Ethics, and to the best of our knowledge, we have not faced any ethical issues during this research. Additionally, all datasets and baselines used in our experiments are freely accessible to the public.

REPRODUCIBILITY STATEMENT

To ensure reproducibility of experiment results throughout the paper, we describe the details of experimental setting and training details in 5.1 and Appendix E, respectively. Furthermore, we provide a source code in <https://anonymous.4open.science/r/CompoDistill-D07F>.

REFERENCES

Shuai Bai, Keqin Chen, Xuejing Liu, Jialin Wang, Wenbin Ge, Sibo Song, Kai Dang, Peng Wang, Shijie Wang, Jun Tang, Humen Zhong, Yuanzhi Zhu, Mingkun Yang, Zhaohai Li, Jianqiang Wan, Pengfei Wang, Wei Ding, Zheren Fu, Yiheng Xu, Jiabo Ye, Xi Zhang, Tianbao Xie, Zesen Cheng, Hang Zhang, Zhibo Yang, Haiyang Xu, and Junyang Lin. Qwen2.5-v1 technical report, 2025. URL <https://arxiv.org/abs/2502.13923>.

Jeffrey P Bigham, Chandrika Jayant, Hanjie Ji, Greg Little, Andrew Miller, Robert C Miller, Robin Miller, Aubrey Tatarowicz, Brandy White, Samual White, et al. Vizwiz: nearly real-time answers to visual questions. In *Proceedings of the 23nd annual ACM symposium on User interface software and technology*, pp. 333–342, 2010.

540 Yuxuan Cai, Jiangning Zhang, Haoyang He, Xinwei He, Ao Tong, Zhenye Gan, Chengjie Wang,
 541 Zhucun Xue, Yong Liu, and Xiang Bai. Llava-kd: A framework of distilling multimodal large
 542 language models. *arXiv preprint arXiv:2410.16236*, 2024.

543

544 Jie Cao and Jing Xiao. An augmented benchmark dataset for geometric question answering through
 545 dual parallel text encoding. In Nicoletta Calzolari, Chu-Ren Huang, Hansaem Kim, James Pustejovsky,
 546 Leo Wanner, Key-Sun Choi, Pum-Mo Ryu, Hsin-Hsi Chen, Lucia Donatelli, Heng Ji,
 547 Sadao Kurohashi, Patrizia Paggio, Nianwen Xue, Seokhwan Kim, Younggyun Hahm, Zhong
 548 He, Tony Kyungil Lee, Enrico Santus, Francis Bond, and Seung-Hoon Na (eds.), *Proceedings
 549 of the 29th International Conference on Computational Linguistics*, pp. 1511–1520, Gyeongju,
 550 Republic of Korea, October 2022. International Committee on Computational Linguistics. URL
 551 <https://aclanthology.org/2022.coling-1.130/>.

552

553 Junbum Cha, Wooyoung Kang, Jonghwan Mun, and Byungseok Roh. Honeybee: Locality-enhanced
 projector for multimodal lilm, 2024. URL <https://arxiv.org/abs/2312.06742>.

554

555 Shiqi Chen, Jinghan Zhang, Tongyao Zhu, Wei Liu, Siyang Gao, Miao Xiong, Manling Li, and
 556 Junxian He. Bring reason to vision: Understanding perception and reasoning through model
 557 merging. *arXiv preprint arXiv:2505.05464*, 2025a.

558

559 Shiqi Chen, Tongyao Zhu, Ruochen Zhou, Jinghan Zhang, Siyang Gao, Juan Carlos Niebles, Mor
 560 Geva, Junxian He, Jiajun Wu, and Manling Li. Why is spatial reasoning hard for vlms? an atten-
 561 tion mechanism perspective on focus areas, 2025b. URL <https://arxiv.org/abs/2503.01773>.

562

563 Zhe Chen, Jiannan Wu, Wenhui Wang, Weijie Su, Guo Chen, Sen Xing, Muyan Zhong, Qinglong
 564 Zhang, Xizhou Zhu, Lewei Lu, Bin Li, Ping Luo, Tong Lu, Yu Qiao, and Jifeng Dai. Internvl:
 565 Scaling up vision foundation models and aligning for generic visual-linguistic tasks, 2024. URL
 566 <https://arxiv.org/abs/2312.14238>.

567

568 Xiangxiang Chu, Limeng Qiao, Xinyu Zhang, Shuang Xu, Fei Wei, Yang Yang, Xiaofei Sun, Yiming
 569 Hu, Xinyang Lin, Bo Zhang, and Chunhua Shen. Mobilevlm v2: Faster and stronger baseline for
 570 vision language model, 2024. URL <https://arxiv.org/abs/2402.03766>.

571

572 Christopher Clark and Matt Gardner. Simple and effective multi-paragraph reading comprehension,
 573 2017. URL <https://arxiv.org/abs/1710.10723>.

574

575 Timothée Darcet, Maxime Oquab, Julien Mairal, and Piotr Bojanowski. Vision transformers need
 576 registers, 2024. URL <https://arxiv.org/abs/2309.16588>.

577

578 Qianhan Feng, Wenshuo Li, Tong Lin, and Xinghao Chen. Align-kd: Distilling cross-modal align-
 579 ment knowledge for mobile vision-language large model enhancement. In *Proceedings of the
 580 Computer Vision and Pattern Recognition Conference*, pp. 4178–4188, 2025.

581

582 Chaoyou Fu, Peixian Chen, Yunhang Shen, Yulei Qin, Mengdan Zhang, Xu Lin, Jinrui Yang, Xiawu
 583 Zheng, Ke Li, Xing Sun, Yunsheng Wu, and Rongrong Ji. Mme: A comprehensive evaluation
 584 benchmark for multimodal large language models, 2024. URL <https://arxiv.org/abs/2306.13394>.

585

586 Yash Goyal, Tejas Khot, Douglas Summers-Stay, Dhruv Batra, and Devi Parikh. Making the v in vqa
 587 matter: Elevating the role of image understanding in visual question answering. In *Proceedings
 588 of the IEEE conference on computer vision and pattern recognition*, pp. 6904–6913, 2017.

589

590 Muyang He, Yixin Liu, Boya Wu, Jianhao Yuan, Yueze Wang, Tiejun Huang, and Bo Zhao. Efficient
 591 multimodal learning from data-centric perspective. *arXiv preprint arXiv:2402.11530*, 2024.

592

593 Geoffrey Hinton, Oriol Vinyals, and Jeff Dean. Distilling the knowledge in a neural network, 2015.
 594 URL <https://arxiv.org/abs/1503.02531>.

595

596 Cheng-Yu Hsieh, Jieyu Zhang, Zixian Ma, Aniruddha Kembhavi, and Ranjay Krishna. Sugarcane:
 597 Fixing hackable benchmarks for vision-language compositionality. *Advances in neural informa-
 598 tion processing systems*, 36:31096–31116, 2023.

594 Shengding Hu, Yuge Tu, Xu Han, Chaoqun He, Ganqu Cui, Xiang Long, Zhi Zheng, Yewei Fang,
 595 Yuxiang Huang, Weilin Zhao, Xinrong Zhang, Zheng Leng Thai, Kaihuo Zhang, Chongyi Wang,
 596 Yuan Yao, Chenyang Zhao, Jie Zhou, Jie Cai, Zhongwu Zhai, Ning Ding, Chao Jia, Guoyang
 597 Zeng, Dahai Li, Zhiyuan Liu, and Maosong Sun. Minicpm: Unveiling the potential of small
 598 language models with scalable training strategies, 2024. URL <https://arxiv.org/abs/2404.06395>.
 599

600 Drew A Hudson and Christopher D Manning. Gqa: A new dataset for real-world visual reasoning
 601 and compositional question answering. In *Proceedings of the IEEE/CVF conference on computer*
 602 *vision and pattern recognition*, pp. 6700–6709, 2019.

603

604 Zhangqi Jiang, Junkai Chen, Beier Zhu, Tingjin Luo, Yankun Shen, and Xu Yang. Devils in middle
 605 layers of large vision-language models: Interpreting, detecting and mitigating object hallucina-
 606 tions via attention lens, 2025. URL <https://arxiv.org/abs/2411.16724>.

607

608 Xiaoqi Jiao, Yichun Yin, Lifeng Shang, Xin Jiang, Xiao Chen, Linlin Li, Fang Wang, and Qun Liu.
 609 Tinybert: Distilling bert for natural language understanding, 2020. URL <https://arxiv.org/abs/1909.10351>.

610

611 Omri Kaduri, Shai Bagon, and Tali Dekel. What’s in the image? a deep-dive into the vision of vision
 612 language models, 2024. URL <https://arxiv.org/abs/2411.17491>.

613

614 Kushal Kafle, Brian Price, Scott Cohen, and Christopher Kanan. Dvqa: Understanding data visual-
 615 izations via question answering, 2018. URL <https://arxiv.org/abs/1801.08163>.

616

617 Seil Kang, Jinyeong Kim, Junhyeok Kim, and Seong Jae Hwang. Your large vision-language model
 618 only needs a few attention heads for visual grounding. In *Proceedings of the Computer Vision*
 and *Pattern Recognition Conference*, pp. 9339–9350, 2025.

619

620 Oğuzhan Fatih Kar, Alessio Tonioni, Petra Poklukar, Achin Kulshrestha, Amir Zamir, and Federico
 621 Tombari. Brave: Broadening the visual encoding of vision-language models, 2024. URL <https://arxiv.org/abs/2404.07204>.

622

623 Aniruddha Kembhavi, Mike Salvato, Eric Kolve, Minjoon Seo, Hannaneh Hajishirzi, and Ali
 624 Farhadi. A diagram is worth a dozen images, 2016. URL <https://arxiv.org/abs/1603.07396>.

625

626 Geewook Kim, Teakgyu Hong, Moonbin Yim, Jeongyeon Nam, Jinyoung Park, Jinyeong Yim, Won-
 627 seek Hwang, Sangdoo Yun, Dongyoon Han, and Seunghyun Park. Ocr-free document under-
 628 standing transformer, 2022. URL <https://arxiv.org/abs/2111.15664>.

629

630 Ranjay Krishna, Yuke Zhu, Oliver Groth, Justin Johnson, Kenji Hata, Joshua Kravitz, Stephanie
 631 Chen, Yannis Kalantidis, Li-Jia Li, David A. Shamma, Michael S. Bernstein, and Fei-Fei Li.
 632 Visual genome: Connecting language and vision using crowdsourced dense image annotations,
 2016. URL <https://arxiv.org/abs/1602.07332>.

633

634 Byung-Kwan Lee, Ryo Hachiuma, Yong Man Ro, Yu-Chiang Frank Wang, and Yueh-Hua Wu. Gen-
 635 recal: Generation after recalibration from large to small vision-language models. *arXiv preprint*
arXiv:2506.15681, 2025a.

636

637 Byung-Kwan Lee, Ryo Hachiuma, Yu-Chiang Frank Wang, Yong Man Ro, and Yueh-Hua Wu. Vlsi:
 638 Verbalized layers-to-interactions from large to small vision language models. In *Proceedings of*
the Computer Vision and Pattern Recognition Conference, pp. 29545–29557, 2025b.

639

640 Bin Lin, Zhenyu Tang, Yang Ye, Jiaxi Cui, Bin Zhu, Peng Jin, Jinfa Huang, Junwu Zhang, Yatian
 641 Pang, Munan Ning, et al. Moe-l lava: Mixture of experts for large vision-language models. *arXiv*
preprint arXiv:2401.15947, 2024a.

642

643 Ji Lin, Hongxu Yin, Wei Ping, Pavlo Molchanov, Mohammad Shoeybi, and Song Han. Vila: On pre-
 644 training for visual language models. In *Proceedings of the IEEE/CVF conference on computer*
 645 *vision and pattern recognition*, pp. 26689–26699, 2024b.

646

647 Haotian Liu, Chunyuan Li, Qingyang Wu, and Yong Jae Lee. Visual instruction tuning, 2023. URL
<https://arxiv.org/abs/2304.08485>.

648 Haotian Liu, Chunyuan Li, Yuheng Li, and Yong Jae Lee. Improved baselines with visual instruction
 649 tuning, 2024. URL <https://arxiv.org/abs/2310.03744>.

650

651 Ilya Loshchilov and Frank Hutter. Decoupled weight decay regularization. *arXiv preprint*
 652 *arXiv:1711.05101*, 2017.

653 Haoyu Lu, Wen Liu, Bo Zhang, Bingxuan Wang, Kai Dong, Bo Liu, Jingxiang Sun, Tongzheng
 654 Ren, Zhusu Li, Hao Yang, Yaofeng Sun, Chengqi Deng, Hanwei Xu, Zhenda Xie, and Chong
 655 Ruan. Deepseek-vl: Towards real-world vision-language understanding, 2024. URL <https://arxiv.org/abs/2403.05525>.

656

657 Pan Lu, Swaroop Mishra, Tony Xia, Liang Qiu, Kai-Wei Chang, Song-Chun Zhu, Oyvind Tafjord,
 658 Peter Clark, and Ashwin Kalyan. Learn to explain: Multimodal reasoning via thought chains for
 659 science question answering, 2022. URL <https://arxiv.org/abs/2209.09513>.

660

661 Teli Ma, Rong Li, and Junwei Liang. An examination of the compositionality of large generative
 662 vision-language models. *arXiv preprint arXiv:2308.10509*, 2023.

663

664 Kenneth Marino, Mohammad Rastegari, Ali Farhadi, and Roozbeh Mottaghi. Ok-vqa: A visual
 665 question answering benchmark requiring external knowledge, 2019. URL <https://arxiv.org/abs/1906.00067>.

666

667 Ahmed Masry, Do Xuan Long, Jia Qing Tan, Shafiq Joty, and Enamul Hoque. Chartqa: A benchmark
 668 for question answering about charts with visual and logical reasoning, 2022. URL <https://arxiv.org/abs/2203.10244>.

669

670 Imanol Miranda, Ander Salaberria, Eneko Agirre, and Gorka Azkune. Bivlc: Extending vision-
 671 language compositionality evaluation with text-to-image retrieval. *Advances in Neural Information
 672 Processing Systems*, 37:101880–101904, 2024.

673

674 Anand Mishra, Shashank Shekhar, Ajeet Kumar Singh, and Anirban Chakraborty. Ocr-vqa: Visual
 675 question answering by reading text in images. In *2019 International Conference on Document
 676 Analysis and Recognition (ICDAR)*, pp. 947–952, 2019. doi: 10.1109/ICDAR.2019.00156.

677

678 Clement Neo, Luke Ong, Philip Torr, Mor Geva, David Krueger, and Fazl Barez. Towards interpreting
 679 visual information processing in vision-language models, 2025. URL <https://arxiv.org/abs/2410.07149>.

680

681 OpenAI. Gpt-4v(ision) technical work and authors, 2023. URL <https://openai.com/contributions/gpt-4v/>. Accessed: 2025-09-18.

682

683 Jianing Qi, Jiawei Liu, Hao Tang, and Zhigang Zhu. Beyond semantics: Rediscovering spatial awareness
 684 in vision-language models, 2025. URL <https://arxiv.org/abs/2503.17349>.

685

686 Qwen, :, An Yang, Baosong Yang, Beichen Zhang, Binyuan Hui, Bo Zheng, Bowen Yu, Chengyuan
 687 Li, Dayiheng Liu, Fei Huang, Haoran Wei, Huan Lin, Jian Yang, Jianhong Tu, Jianwei Zhang,
 688 Jianxin Yang, Jiaxi Yang, Jingren Zhou, Junyang Lin, Kai Dang, Keming Lu, Keqin Bao, Kexin
 689 Yang, Le Yu, Mei Li, Mingfeng Xue, Pei Zhang, Qin Zhu, Rui Men, Runji Lin, Tianhao Li, Tianyi
 690 Tang, Tingyu Xia, Xingzhang Ren, Xuancheng Ren, Yang Fan, Yang Su, Yichang Zhang, Yu Wan,
 691 Yuqiong Liu, Zeyu Cui, Zhenru Zhang, and Zihan Qiu. Qwen2.5 technical report, 2025. URL
<https://arxiv.org/abs/2412.15115>.

692

693 Alec Radford, Jong Wook Kim, Chris Hallacy, Aditya Ramesh, Gabriel Goh, Sandhini Agarwal,
 694 Girish Sastry, Amanda Askell, Pamela Mishkin, Jack Clark, et al. Learning transferable visual
 695 models from natural language supervision. In *International conference on machine learning*, pp.
 8748–8763. PMLR, 2021.

696

697 Ahmad Sajedi, Samir Khaki, Ehsan Amjadian, Lucy Z Liu, Yuri A Lawryshyn, and Konstantinos N
 698 Plataniotis. Datadam: Efficient dataset distillation with attention matching. In *Proceedings of the
 699 IEEE/CVF International Conference on Computer Vision*, pp. 17097–17107, 2023.

700

701 Dustin Schwenk, Apoorv Khandelwal, Christopher Clark, Kenneth Marino, and Roozbeh Mottaghi. A-okvqa: A benchmark for visual question answering using world knowledge, 2022. URL
<https://arxiv.org/abs/2206.01718>.

702 Zhenwei Shao, Zhou Yu, Jun Yu, Xuecheng Ouyang, Lihao Zheng, Zhenbiao Gai, Mingyang Wang,
 703 Zhenzhong Kuang, and Jiajun Ding. Imp: Highly capable large multimodal models for mobile
 704 devices. *IEEE Transactions on Multimedia*, 2025.

705

706 Fangxun Shu, Yue Liao, Le Zhuo, Chenning Xu, Lei Zhang, Guanghao Zhang, Haonan Shi, Long
 707 Chen, Tao Zhong, Wanggui He, et al. Llava-mod: Making llava tiny via moe knowledge distilla-
 708 tion. *arXiv preprint arXiv:2408.15881*, 2024.

709

710 Amanpreet Singh, Vivek Natarajan, Meet Shah, Yu Jiang, Xinlei Chen, Dhruv Batra, Devi Parikh,
 711 and Marcus Rohrbach. Towards vqa models that can read. In *Proceedings of the IEEE/CVF*
 712 conference on computer vision and pattern recognition, pp. 8317–8326, 2019.

713

714 Siqi Sun, Yu Cheng, Zhe Gan, and Jingjing Liu. Patient knowledge distillation for bert model
 715 compression, 2019. URL <https://arxiv.org/abs/1908.09355>.

716

717 Tristan Thrush, Ryan Jiang, Max Bartolo, Amanpreet Singh, Adina Williams, Douwe Kiela, and
 718 Candace Ross. Winoground: Probing vision and language models for visio-linguistic composi-
 719 tionality. In *Proceedings of the IEEE/CVF Conference on Computer Vision and Pattern Recog-
 720 nition*, pp. 5238–5248, 2022.

721

722 Shengbang Tong, Zhuang Liu, Yuexiang Zhai, Yi Ma, Yann LeCun, and Saining Xie. Eyes wide
 723 shut? exploring the visual shortcomings of multimodal llms, 2024. URL <https://arxiv.org/abs/2401.06209>.

724

725 Ashish Vaswani, Noam Shazeer, Niki Parmar, Jakob Uszkoreit, Llion Jones, Aidan N Gomez,
 726 Łukasz Kaiser, and Illia Polosukhin. Attention is all you need. *Advances in neural information
 727 processing systems*, 30, 2017.

728

729 Weihan Wang, Qingsong Lv, Wenmeng Yu, Wenyi Hong, Ji Qi, Yan Wang, Junhui Ji, Zhuoyi Yang,
 730 Lei Zhao, Xixuan Song, Jiazheng Xu, Bin Xu, Juanzi Li, Yuxiao Dong, Ming Ding, and Jie Tang.
 731 Cogvlm: Visual expert for pretrained language models, 2024. URL <https://arxiv.org/abs/2311.03079>.

732

733 Wenhui Wang, Furu Wei, Li Dong, Hangbo Bao, Nan Yang, and Ming Zhou. Minilm: Deep
 734 self-attention distillation for task-agnostic compression of pre-trained transformers, 2020. URL
 735 <https://arxiv.org/abs/2002.10957>.

736

737 Mingrui Wu, Jiayi Ji, Oucheng Huang, Jiale Li, Yuhang Wu, Xiaoshuai Sun, and Rongrong Ji.
 738 Evaluating and analyzing relationship hallucinations in large vision-language models, 2024. URL
 739 <https://arxiv.org/abs/2406.16449>.

740

741 Shilin Xu, Xiangtai Li, Haobo Yuan, Lu Qi, Yunhai Tong, and Ming-Hsuan Yang. Llavadi: What
 742 matters for multimodal large language models distillation. *arXiv preprint arXiv:2407.19409*,
 743 2024.

744

745 An Yang, Baosong Yang, Binyuan Hui, Bo Zheng, Bowen Yu, Chang Zhou, Chengpeng Li,
 746 Chengyuan Li, Dayiheng Liu, Fei Huang, Guanting Dong, Haoran Wei, Huan Lin, Jialong Tang,
 747 Jialin Wang, Jian Yang, Jianhong Tu, Jianwei Zhang, Jianxin Ma, Jianxin Yang, Jin Xu, Jin-
 748 gren Zhou, Jinze Bai, Jinzheng He, Junyang Lin, Kai Dang, Keming Lu, Keqin Chen, Kexin
 749 Yang, Mei Li, Mingfeng Xue, Na Ni, Pei Zhang, Peng Wang, Ru Peng, Rui Men, Ruize Gao,
 750 Runji Lin, Shijie Wang, Shuai Bai, Sinan Tan, Tianhang Zhu, Tianhao Li, Tianyu Liu, Wen-
 751 bin Ge, Xiaodong Deng, Xiaohuan Zhou, Xingzhang Ren, Xinyu Zhang, Xipin Wei, Xuancheng
 752 Ren, Xuejing Liu, Yang Fan, Yang Yao, Yichang Zhang, Yu Wan, Yunfei Chu, Yuqiong Liu,
 753 Zeyu Cui, Zhenru Zhang, Zhifang Guo, and Zhihao Fan. Qwen2 technical report, 2024. URL
 754 <https://arxiv.org/abs/2407.10671>.

755

756 Heeji Yoon, Jaewoo Jung, Junwan Kim, Hyungyu Choi, Heeseong Shin, Sangbeom Lim, Honggyu
 757 An, Chaehyun Kim, Jisang Han, Donghyun Kim, Chanho Eom, Sunghwan Hong, and Seungry-
 758 ong Kim. Visual representation alignment for multimodal large language models, 2025. URL
 759 <https://arxiv.org/abs/2509.07979>.

760

761 Licheng Yu, Patrick Poirson, Shan Yang, Alexander C. Berg, and Tamara L. Berg. Modeling context
 762 in referring expressions, 2016. URL <https://arxiv.org/abs/1608.00272>.

756 Xiaohua Zhai, Basil Mustafa, Alexander Kolesnikov, and Lucas Beyer. Sigmoid loss for language
757 image pre-training. In *Proceedings of the IEEE/CVF international conference on computer vision*,
758 pp. 11975–11986, 2023.

759 Tianyang Zhao, Kunwar Yashraj Singh, Srikanth Appalaraju, Peng Tang, Vijay Mahadevan, R Man-
760 matha, and Ying Nian Wu. No head left behind–multi-head alignment distillation for transfor-
761 mers. In *Proceedings of the AAAI Conference on Artificial Intelligence*, volume 38, pp. 7514–7524,
762 2024.

763 Kening Zheng, Junkai Chen, Yibo Yan, Xin Zou, and Xuming Hu. Reefknot: A comprehensive
764 benchmark for relation hallucination evaluation, analysis and mitigation in multimodal large lan-
765 guage models, 2025. URL <https://arxiv.org/abs/2408.09429>.

766 Yang Zhou, Xu Gao, Zichong Chen, and Hui Huang. Attention distillation: A unified approach to
767 visual characteristics transfer. In *Proceedings of the Computer Vision and Pattern Recognition
768 Conference*, pp. 18270–18280, 2025.

770

771

772

773

774

775

776

777

778

779

780

781

782

783

784

785

786

787

788

789

790

791

792

793

794

795

796

797

798

799

800

801

802

803

804

805

806

807

808

809

810 811 812 813 814 815 816 817 818 819 *Supplementary Material*

820
821 *- CompoDistill: Attention Distillation for
822 Compositional Reasoning in Multimodal LLMs -*

A Additional Visualizations on Attention Misalignment	18
B Differences between Visual Recognition and Perception Abilities	18
B.1 Visual Recognition	19
B.2 Visual Perception	20
C Additional Experiments on Attention Similarity	20
D Baseline Methods	20
E Additional Implementation Details	21
E.1 Training Strategy and Hyper-parameters	21
F Explanation of the Baselines for Layer Matching Strategy	22
G Explanation for the Extended Training Data	22
H Additional Experiments Results	23
H.1 Detailed Experiment Results on VAT module	23
H.1.1 Detailed Experiment Results on Attention Loss Type	23
H.1.2 Detailed Experiment Results on Attention Target Layers	23
H.1.3 Detailed Experiment Results on Layers Matching Strategy	24
H.2 Detailed Experiment Results on Relational Hallucination	24
H.3 (Additional) Detailed Experiments Results on Training Strategy.	24
H.4 Detailed Experiments Results on Scalability	25
H.4.1 Detailed Experiments Results on Data Scaling	25
H.4.2 Detailed Experiments Results on Student and Teacher LLM Size	25
H.4.3 Detailed Experiments Results on different LLM Backbones	26
I Generalization to Other Architecture	26
J Discussion about Training Overhead	27
K Additional Experiment on Attention Mixing	28
L Additional Experiment on Teacher Adapter Fetch Module	28
M Additional Experiment on Visual ATtension Alignment Module	29

864	N Discussion on Possibility about Teacher Overfitting	29
865		
866	O Additional Experiment on Visual Grounding	30
867		
868	P Limitation and Future work	31
870		
871		
872		
873		
874		
875		
876		
877		
878		
879		
880		
881		
882		
883		
884		
885		
886		
887		
888		
889		
890		
891		
892		
893		
894		
895		
896		
897		
898		
899		
900		
901		
902		
903		
904		
905		
906		
907		
908		
909		
910		
911		
912		
913		
914		
915		
916		
917		

918 A ADDITIONAL VISUALIZATIONS ON ATTENTION MISALIGNMENT
919

920 In this section, we provide additional qualitative examples of the **attention misalignment** between
921 the student and the teacher model, a concept introduced in Section 1. To facilitate comprehension,
922 we have highlighted crucial textual components in **red**, specifically phrases that require relational un-
923 derstanding or accurate attribute recognition. For a comprehensive comparison, we present results
924 for an additional student model (LLaVADI-2B) and our method (**CompoDistill**), alongside the base-
925 line LLaVA-KD-2B and LLaVA-4B (Teacher). Notably, the visualizations show that **CompoDistill**
926 produces an attention map remarkably similar to the teacher’s, correctly focusing on the key visual
927 areas relevant to the text. These comparisons are illustrated in Figure 6 and Figure 7.

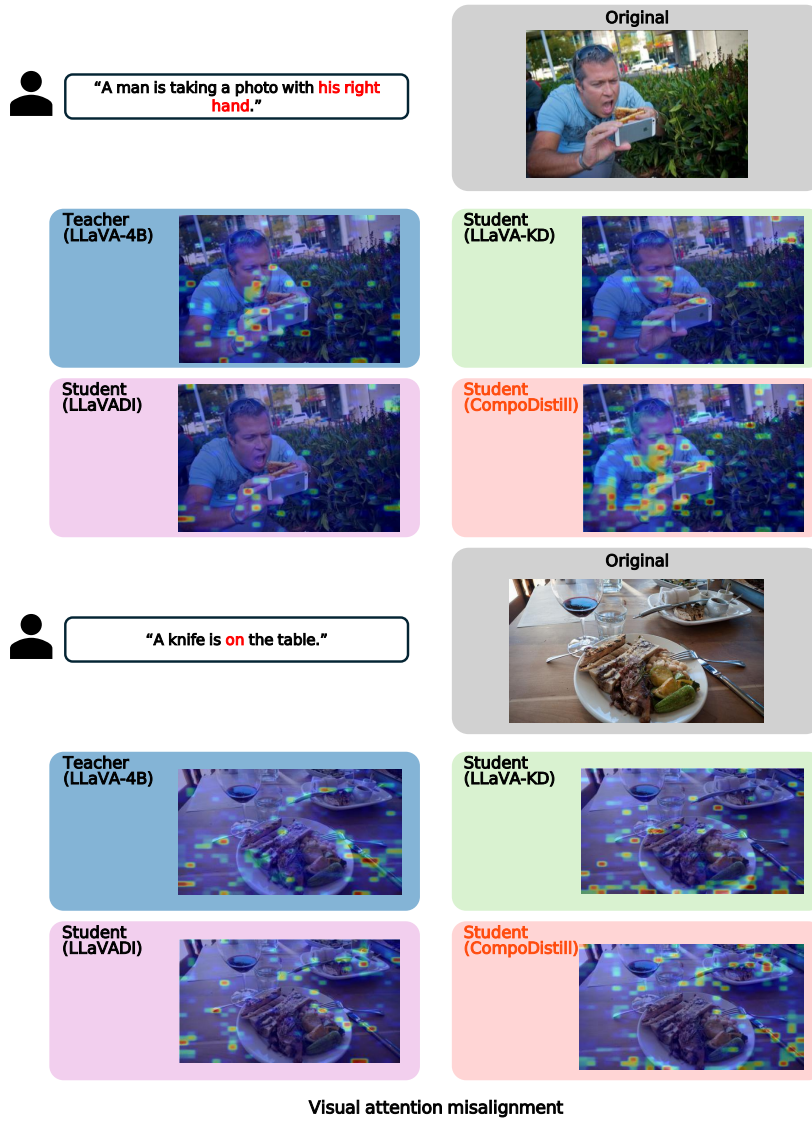


Figure 6: Examples of attention misalignment.

967 B DIFFERENCES BETWEEN VISUAL RECOGNITION AND PERCEPTION
968 ABILITIES
969

970 This section provides a detailed explanation of the distinction between visual recognition and visual
971 perception abilities, which are evaluated using Visual Question Answering (VQA) and Composi-

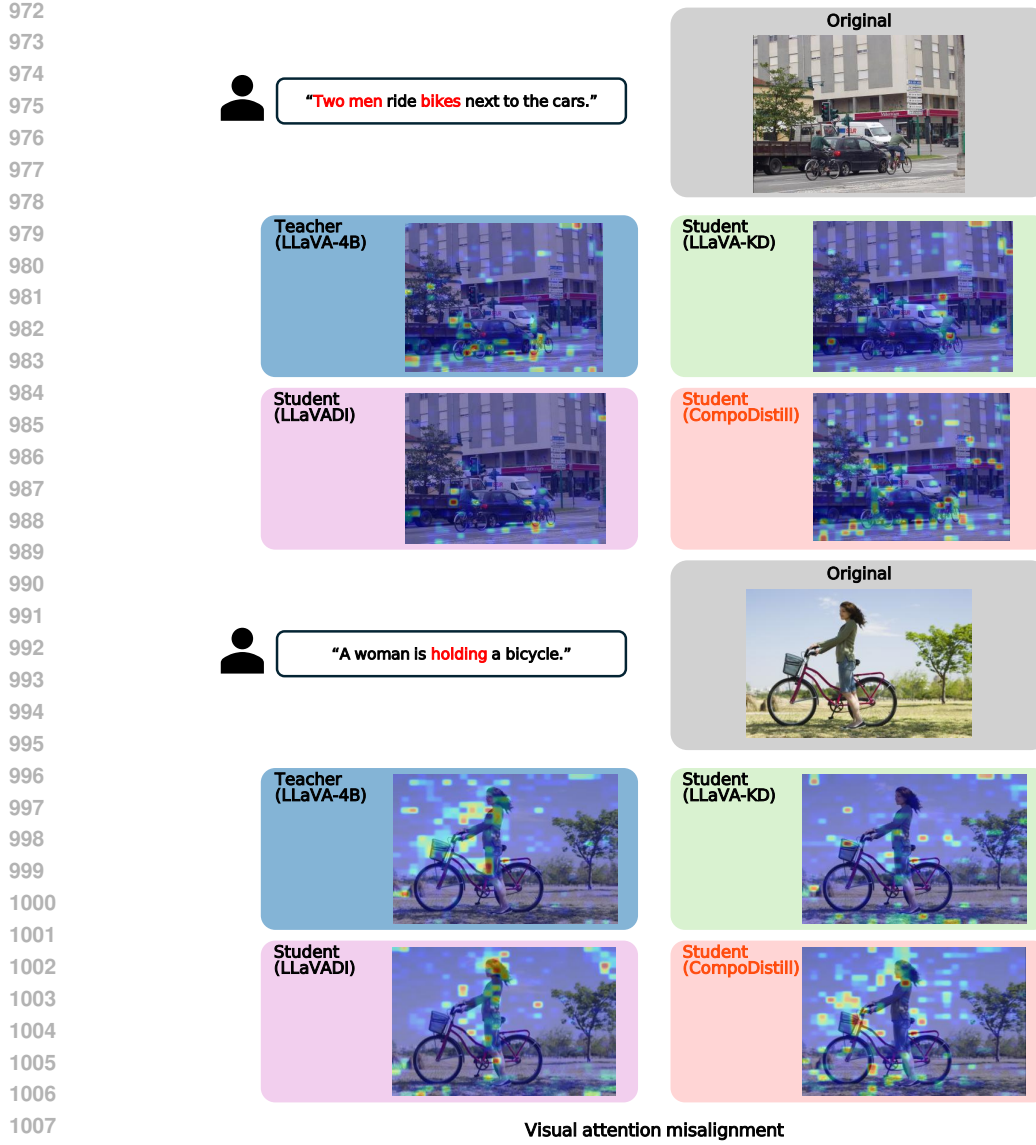


Figure 7: Examples of attention misalignment.

tional Reasoning (CR) datasets, respectively. Also in Figure 8, we illustrated an example of VQA and CR question.

B.1 VISUAL RECOGNITION

Visual recognition is the foundational ability of a model to **identify and categorize objects, scenes, and their basic attributes within an image**. It fundamentally answers the question, such as “What is in this image?: This process relies on matching learned visual patterns—such as textures, shapes, and colors—to specific labels or concepts. For example, when a model identifies a four-legged furry animal as a “dog”, it is performing visual recognition. This ability is analogous to building a vocabulary of the visual world.

Most standard VQA datasets (e.g., VQAv2 (Goyal et al., 2017), Vizwiz (Bigham et al., 2010), and GQA (Hudson & Manning, 2019)) are primarily designed to evaluate this recognition capability. The questions in these datasets are typically direct and fact-based, probing for the presence, count, or simple properties of objects. They can often be answered correctly if the model successfully

1026

1027

1028

1029

1030

1031

1032

1033

1034

1035

1036

1037

1038

1039

1040

1041

1042

1043

1044

1045

1046

1047

1048

1049

1050

1051

1052

1053

1054

1055

1056

1057

1058

1059

1060

1061

1062

1063

1064

1065

1066

1067

1068

1069

1070

1071

1072

1073

1074

1075

1076

1077

1078

1079

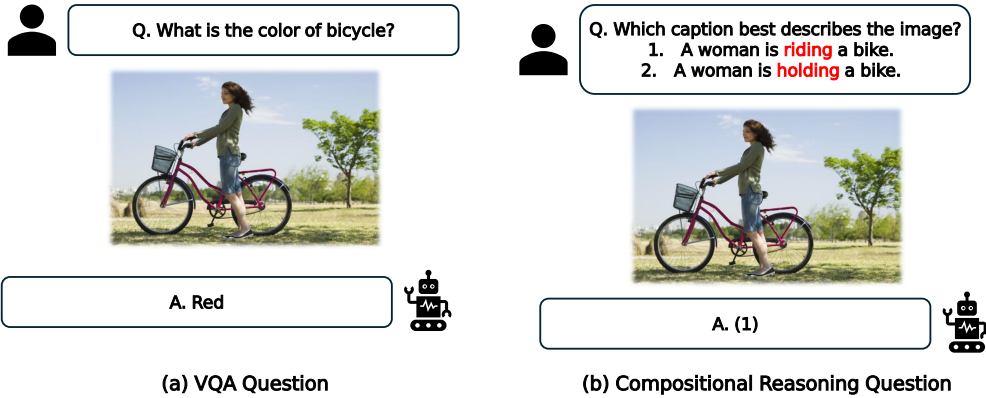


Figure 8: An example of a standard VQA question, which requires simple object identification, versus a Compositional Reasoning (CR) question, which requires accurately distinguishing between two detailed and confusable multiple choices.

recognizes the key objects and their most salient features, without needing to understand complex inter-object relationships.

B.2 VISUAL PERCEPTION

Visual perception is a more advanced cognitive ability that goes beyond simple identification. It involves **interpreting and understanding the relationships between objects, their precise attributes, their spatial arrangement, and the overall context of the scene**. If recognition is about what, perception is about how and why such as how objects are arranged, how they interact, and why the scene is composed in a particular way. This requires the model to not just list the contents of an image, but to build a coherent, structured understanding of it.

Compositional Reasoning (CR) datasets are specifically designed to evaluate this perceptual ability. The questions are structured to be challenging for models that rely solely on simple keyword matching or recognition. To answer correctly, a model must accurately bind specific attributes to their corresponding objects and correctly interpret the spatial or semantic relationships between them. These questions often test a model’s robustness where the correct objects and attributes are present but not in the configuration described by the question.

C ADDITIONAL EXPERIMENTS ON ATTENTION SIMILARITY

To further validate our findings in Section 3.1, we extend our attention similarity analysis to two additional benchmark datasets: VQAv2 (Goyal et al., 2017) for VQA and Winoground (Thrush et al., 2022) for CR, replicating the experimental setup used for GQA (Hudson & Manning, 2019) and SugarCrepe (Hsieh et al., 2023).

The results, visualized in Figure 9, demonstrate a consistent trend with the conclusions drawn in our main analysis. The analysis reaffirms the critical role of attention over visual tokens in performance improvement. Specifically, on the Winoground (Thrush et al., 2022) (CR) task, where the student model’s performance gain over the SFT baseline was marginal, we again observe no significant increase in teacher-student attention similarity. This result corroborates our main argument that higher attention similarity over visual tokens in the visual understanding layers is a key factor for the effective distillation of visual perception.

D BASELINE METHODS

We include several baselines from two main groups. The first group consists of Knowledge Distillation-based methods, including LLaVADI-2B (Xu et al., 2024), LLaVA-KD-2B (Cai et al., 2024), and LLaVA-MoD-2B (Shu et al., 2024). **To ensure fair comparisons, all KD models were dis-**

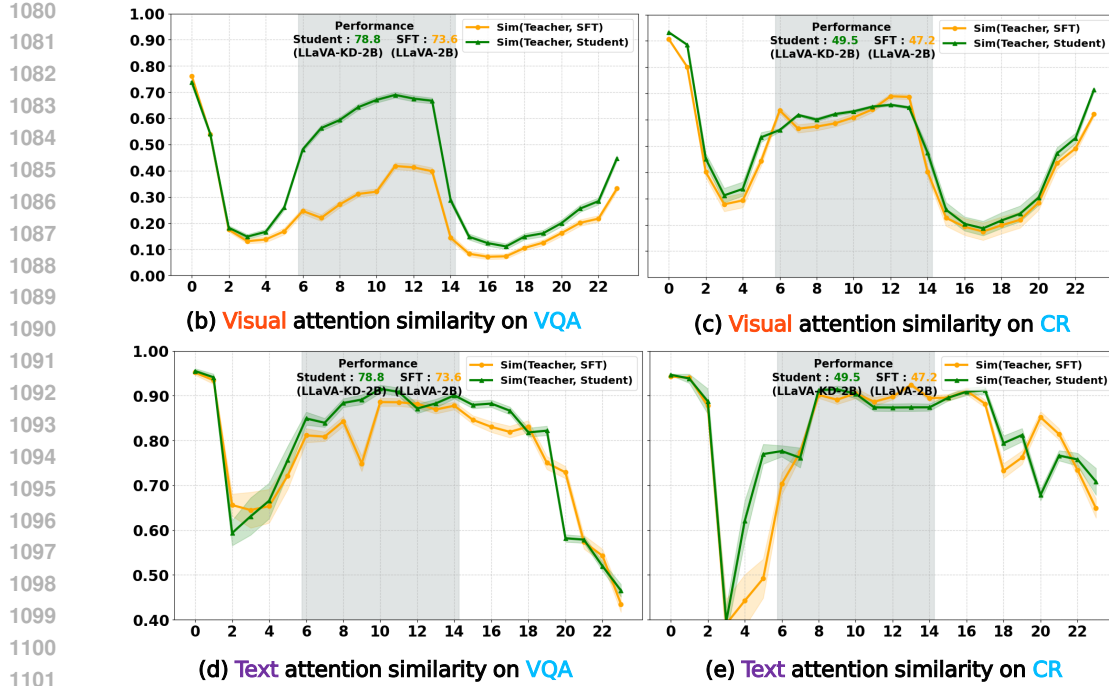


Figure 9: Layerwise attention similarity of visual tokens and text tokens between student/SFT models and the teacher model.

tilled from the same teacher model (i.e., LLaVA-4B) and share the same LLM backbone (i.e., **Qwen 1.5**). The second group comprises a broad range of General MLLMs with parameter sizes in the range of 1.3B–3B, comparable to that of the compared KD methods, for direct performance comparison. This includes models such as Imp-2B (Shao et al., 2025), Bunny-2B (He et al., 2024), MoE-LLaVA-2B (Lin et al., 2024a), LLaVA-2B (Liu et al., 2024), and Deepseek-VL-1.3B (Lu et al., 2024), MobileVLM-1.7B (Chu et al., 2024), as well as larger models (4B–7B) like MiniCPM-V-2.4B (Hu et al., 2024), CogVLM-7B (Wang et al., 2024) and Qwen2.5-VL-7B (Bai et al., 2025) to provide state-of-the-art context.

E ADDITIONAL IMPLEMENTATION DETAILS

E.1 TRAINING STRATEGY AND HYPER-PARAMETERS

Our model is initialized with a SigLIP-B/14@384 vision encoder and a Qwen1.5-1.8B LLM. For adapter, we use 3-layer MLP. Across all training stages, we use a consistent setup: Each stage is trained for one epoch using AdamW optimizer (Loshchilov & Hutter, 2017). The AdamW optimizer with $\beta_1 = 0.9$ and $\beta_2 = 0.98$, a cosine decay learning rate scheduler, a weight decay of 0.0, and a warm-up ratio of 0.03. We process images at a resolution of 384x384, with input sequence lengths of 729 for the vision encoder and 2048 for the LLM. All training is performed with Float16 numerical precision and Zero2 model parallelism with 8 NVIDIA L40S 48GB GPUs. For the DPT stage, we use the LLaVA-1.5-558K (Liu et al., 2024) dataset with a batch size of 256 and a learning rate of 1e-3. For the DFT and SFT stages, we use the LLaVA-mix-665K (Liu et al., 2024) dataset with a batch size of 128 and a learning rate of 1e-4.

Our training is divided into three distinct stages, each lasting for one epoch:

Distilled Pre-Training (DPT): In this initial stage, our primary goal is to align the visual representations with the language embedding space. To achieve this, we freeze both the vision encoder and the LLM, and exclusively optimize the parameters of the adapter. This stage uses a global batch size of 256.

1134 Distilled Fine-Tuning (DFT): The scope of training is expanded in the second stage to distill knowl-
 1135 edge more deeply into the language model. The vision encoder remains frozen, but we now co-
 1136 optimize both the LLM and the adapter. For this stage, the global batch size is reduced to 128.
 1137

1138 Supervised Fine-Tuning (SFT): In the final stage, the model, initialized from the DFT checkpoint, is
 1139 further refined. The training configuration mirrors the DFT stage: the vision encoder is frozen, while
 1140 the LLM and adapter are co-optimized. This stage also uses a global batch size of 128 to complete
 1141 the training process.
 1142

1143 The detailed training hyper-parameters are show in Table 8.
 1144

1145 Table 8: Training hyper-parameters of each stage.
 1146

1145 Configuration	1146 Distilled Pre-Training	1147 Distilled Fine-Tuning	1148 Supervised Fine-Tuning
1149 LLM	1150 ✗	1151 ✗	1152 ✗
1153 Vision Encoder	1154 ✗	1155 ✗	1156 ✗
1157 Adapter	1158 ✗	1159 ✗	1160 ✗
1161 LLM init.	1162 Qwen1.5-1.8B	1163 Qwen1.5-1.8B	1164 From DFT
1165 Vision Encoder init.	1166	1167 SigLIP-B/14@384	1168
1169 Image resolution	1170	1171 384 x 384	1172
1173 Vision Encoder Sequence length	1174	1175 729	1176
1177 LLM sequence length	1178	1179 2048	1180
1181 Optimizer	1182	1183 AdamW	1184
1185 Optimizer hyper-parameter	1186	1187 $\beta_1 = 0.9, \beta_2 = 0.98$	1188
1189 Learning rate	1190	1191 2e-4	1192
1193 Learning rate scheduler	1194	1195 Cosine decay	1196
1197 Weight decay	1198	1199 0.0	1200
1201 Training epoch	1202	1203 1.0	1204
1206 Warm-up ratio	1207	1208 0.03	1209
1212 Global batch size	1213 256	1214 128	1215 128
1218 Numerical precision	1219	1220 Float16	1221
1225 Model parallelism	1226	1227 Zero2	1228

1162 F EXPLANATION OF THE BASELINES FOR LAYER MATCHING STRATEGY

1163 In this section, we provide a detailed explanation of the different layer matching strategies evaluated
 1164 in our main ablation study (Table 3c). Layer matching is a critical component of attention distillation,
 1165 as it defines the correspondence between teacher and student layers for knowledge transfer. While
 1166 our proposed method, **Group matching**, proved to be the most effective, we also explored two
 1167 alternative baseline strategies to thoroughly investigate the design space. We will describe each of
 1168 these in turn:
 1169

1170 First, **Simple matching**, a straightforward approach that uniformly samples teacher layers to match
 1171 the number of student layers. Second, **Adaptive matching**. Expanding on (Lee et al., 2025b), this
 1172 method first computes a matrix of Kullback-Leibler (KL) distances between every student target
 1173 layer and every teacher target layer. Each student layer is then greedily paired with the teacher layer
 1174 that has the minimum KL distance, under a consecutive constraint. This constraint ensures that a
 1175 given student layer can only select a teacher layer that comes after the one selected by the previous
 1176 student layer, thereby maintaining the sequential integrity of the model’s architecture.
 1177

1178 G EXPLANATION FOR THE EXTENDED TRAINING DATA

1179 This section provides detailed information on the training data used for the data scaling component
 1180 of our main scalability experiments. Our baseline training utilizes a base dataset of approximately
 1181 1.2M samples, comprising the **LLaVA-1.5-558K** (Liu et al., 2024) for Distilled Pre-Training (DPT)
 1182 and **LLaVA-mix-665K** (Liu et al., 2024) for the Distilled Fine-Tuning (DFT) and Supervised Fine-
 1183 Tuning (SFT) stages.
 1184

1185 To scale the data in Sec 6, we incorporate an additional 1.2M samples, originally curated for the
 1186 Dense-to-Sparse Distillation (D2S) in LLaVA-MoD (Shu et al., 2024). As detailed in Table 9, this
 1187 extended dataset is a diverse mixture covering a wide range of tasks, including General QA, Ground-
 1188 ing, Science, Chart & Document understanding, OCR, and Knowledge-based reasoning.
 1189

1188
1189
1190 Table 9: Training dataset of scaling data experiment.
1191
1192
1193
1194
1195
1196
1197
1198
1199
1200

Stage	Task	Dataset
Distilled Pre-Training (DPT)	Captioning	LLaVA-1.5-558K (Liu et al., 2024)
Distilled Fine-Tuning (DFT)	Conversation	LLaVA-mix-665K (Liu et al., 2024)
Supervised Fine-Tuning (SFT)	Conversation	LLaVA-mix-665K (Liu et al., 2024)
Data Scaling Experiment	Captioning	ShareGPT4V-100K, TextCaps
	Conversation	LLaVA-mix-665K (Liu et al., 2024)
	General QA	GQA (Hudson & Manning, 2019), VQAv2 (Goyal et al., 2017), OKVQA (Marino et al., 2019)
	Grounding	VG (Krishna et al., 2016), RefCoCo (Yu et al., 2016)
	Science	AI2D (Kembhavi et al., 2016), ScienceQA (Lu et al., 2022)
	Chart & Doc	DVQA (Kafle et al., 2018), ChartQA (Masry et al., 2022), DocQA (Clark & Gardner, 2017)
	OCR	OCRVQA (Mishra et al., 2019), SynthDoG-EN (Kim et al., 2022)
	Knowledge	A-OKVQA (Schwenk et al., 2022), GeoQA+ (Cao & Xiao, 2022)

1201
1202 H ADDITIONAL EXPERIMENTS RESULTS
1203
12041205 H.1 DETAILED EXPERIMENT RESULTS ON VAT MODULE
1206
12071208 H.1.1 DETAILED EXPERIMENT RESULTS ON ATTENTION LOSS TYPE
1209
12101211 Table 10: Ablation for various attention loss type.
1212
1213

Attention Loss Type	Attention Matching	Attention Layers	Visual Question Answering				Compositional Reasoning			
			GQA	TextVQA	MME	Avg	Sugarcreepe	SADE	BiVLC	Winoground
<i>Ablation on attention loss type</i>										
MSE.	w/o Attention Loss	Group	intermediate	60.8	56.5	66.5	61.3	78.0	67.0	62.4
KL. Div.		Group	intermediate	59.9	55.3	65.7	60.3	79.9	68.3	62.8
Cos. Sim.		Group	intermediate	60.7	55.6	65.9	60.7	80.1	67.9	63.5
				62.2	56.4	70.1	62.9	82.9	69.4	63.3
									51.1	66.7

1214
1215
1216 We provide a detailed analysis of the impact of different attention loss functions, as summarized
1217 in Table 10. Our goal was to determine the most effective way to quantify the difference between
1218 student and teacher attention maps for distillation. The results show that while all tested loss func-
1219 tions improve performance on Compositional Reasoning (CR) tasks over the baseline, their effects
1220 on Visual Question Answering (VQA) are mixed. Notably, both Mean Squared Error (MSE) and KL
1221 Divergence (KL. Div.) slightly degrade VQA performance.1222
1223 Cosine Similarity (Cos. Sim.) proved to be the most effective loss function, improving performance
1224 across both the VQA and CR domains. We believe this is because it is more crucial for the student
1225 model to learn the relative importance of different visual patches, rather than replicating the exact
1226 absolute values (MSE) or the probability distribution (KL. Div.) of the teacher’s attention scores.1227 H.1.2 DETAILED EXPERIMENT RESULTS ON ATTENTION TARGET LAYERS
1228
12291230 Table 11: Ablation for attention target layers.
1231
1232

Attention Loss Type	Attention Matching	Attention Layers	Visual Question Answering				Compositional Reasoning			
			GQA	TextVQA	MME	Avg	Sugarcreepe	SADE	BiVLC	Winoground
<i>Ablation on target layers for attention distillation</i>										
Cos. Sim.	Group	early (~ 30%)	61.3	55.5	66.8	61.2	80.9	67.4	59.8	46.7
Cos. Sim.	Group	later (70% ~)	61.2	55.7	68.4	61.7	81.8	66.8	59.7	50.0
Cos. Sim.	Group	all	62.1	55.8	69.1	62.4	83.1	68.6	63.7	50.4
Cos. Sim.	Group	intermediate	62.2	56.4	70.1	62.9	82.9	69.4	63.3	51.1
										66.7

1235
1236 We investigate which layers are the most effective targets for attention distillation, with detailed
1237 results in Table 11. We compared four strategies: distilling from early layers (~30%), later layers
1238 (70%~), all layers, and our primary approach of targeting the intermediate layers (**visual under-**
1239 **standing layers**).1240
1241 The results clearly indicate that targeting the visual understanding layers yields the best overall per-
1242 formance on both VQA and CR tasks. While distilling from all layers provides strong and sometimes
1243 comparable results, this approach is less computationally efficient. The more focused intermediate

1242 strategy ultimately achieves a better trade-off, slightly outperforming the all-layer approach in over-
 1243 all scores without the associated computational overhead. Conversely, targeting only the early or
 1244 later layers leads to a noticeable drop in performance.

1245 This confirms our analysis that the intermediate layers, which function as the core **visual under-**
 1246 **standing layers**, are the most critical for visual-semantic integration. Distilling specifically from
 1247 this block provides the most potent and effective signal for knowledge transfer, a finding consistent
 1248 with prior research (Kaduri et al., 2024; Neo et al., 2025).

1250 H.1.3 DETAILED EXPERIMENT RESULTS ON LAYERS MATCHING STRATEGY

1252 Table 12: Ablation for attention matching strategy.

1254 Attention Loss Type	1255 Attention Matching	1256 Attention Layers	1257 Visual Question Answering				1258 Compositional Reasoning			
			GQA	TextVQA	MME	Avg	Sugarcreep	SADE	BiVLC	Winoground
<i>Ablation on layers matching for attention distillation</i>										
Cos. Sim.	Simple	intermediate	60.2	56.3	68.0	61.5	81.6	67.1	63.2	50.7
Cos. Sim.	Adaptive	intermediate	61.4	55.9	68.6	62.0	82.1	68.3	62.8	49.5
Cos. Sim.	Group	intermediate	62.2	56.4	70.1	62.9	82.9	69.4	63.3	51.1
										65.7

1259 This part details our ablation on different strategies for matching student and teacher layers, with
 1260 full results in Table 12 and detailed explanation about each strategy is in Section F. We compared
 1261 our proposed **Group matching** against two strong baselines: **Simple matching** (uniform sampling
 1262 of teacher layers) and **Adaptive matching** (pairing based on feature distance). The data shows that
 1263 while both Simple and Adaptive strategies improve performance over a no-distillation baseline, our
 1264 Group matching consistently achieves the best results across all benchmarks. Notably, our method
 1265 demonstrates a clear performance advantage over the next best method, Adaptive matching. Further-
 1266 more, our approach is more computationally efficient, as it avoid the complex calculations required
 1267 to dynamically match layers inherent to adaptive strategies. This suggests that grouping layers pro-
 1268 vides a more stable and robust signal for the student. By averaging the behavior of a block of teacher
 1269 layers, our method likely smooths out layer-specific idiosyncrasies and transfers a more generalized
 1270 attention strategy.

1271 H.2 DETAILED EXPERIMENT RESULTS ON RELATIONAL HALLUCINATION

1273 Table 13: Relational Hallucination Experiment.

1275 Model	1276 R-Bench			1277 Reefknot		
	Precision	Recall	F1 Score	Perception	Cognitive	Total
Teacher (LLaVA-4B)	66.4	97.8	79.1	45.3	78.0	67.9
Student (LLaVA-4B)	60.5	96.3	74.3	40.1	70.8	61.3
LLaVA-KD-2B	63.5	96.2	76.5	41.8	68.8	60.3
LLaVA-MoD-2B	62.5	97.6	76.2	42.0	73.1	63.4
CompoDistill-2B	65.7	97.6	78.6	43.2	77.3	67.9

1281 As mentioned in the main text, we conducted experiments on relational hallucination benchmarks
 1282 to demonstrate a further benefit of our proposed method. Table 13 presents the detailed quantita-
 1283 tive results of this evaluation on the R-Bench (Wu et al., 2024) and Reefknot (Zheng et al., 2025)
 1284 benchmarks.

1285 The results substantiate our claim, showing that **CompoDistill** significantly outperforms other
 1286 knowledge distillation methods on the R-Bench benchmark and nearly closes the performance gap to
 1287 the teacher model. More strikingly, on the Reefknot benchmark, our method achieves performance
 1288 on par with the teacher model, showcasing its ability to handle complex relational challenges. These
 1289 findings provide strong evidence that enhancing visual perception via **CompoDistill** effectively mit-
 1290 igates relational hallucinations and boosts performance on complex visual reasoning tasks.

1292 H.3 (ADDITIONAL) DETAILED EXPERIMENTS RESULTS ON TRAINING STRATEGY.

1294 In this section, we provide additional experimental results to analyze the effectiveness of our pro-
 1295 posed three-stage training strategy (DPT-DFT-SFT). To demonstrate its efficacy, we investigate the
 1296 specific impact of each individual stage, with detailed results presented in Table 14.

1296 First, the Distilled Pre-Training (DPT) stage shows a significant impact, particularly on Visual Ques-
 1297 tion Answering (VQA) tasks. As seen by comparing configurations with and without DPT (e.g., (1)
 1298 vs. (3)), replacing standard pre-training with our distilled approach consistently yields substantial
 1299 improvements in VQA scores. This highlights DPT’s role in building a strong visual knowledge
 1300 from the teacher.

1301 Next, the Distilled Feature-Tuning (DFT) stage is crucial for enhancing Compositional Reasoning
 1302 (CR) capabilities. The inclusion of DFT leads to the most significant gains in CR performance across
 1303 all benchmarks. We attribute this improvement to the effective transfer of the teacher’s fine-grained
 1304 attention patterns through our attention distillation process, which is vital for understanding complex
 1305 object relationships.

1306 Finally, the Supervised Fine-Tuning (SFT) stage is indispensable. The results from the configuration
 1307 without SFT (4) show a catastrophic failure on VQA tasks, as the model completely fails to follow
 1308 task instructions. This demonstrates that SFT is an absolutely critical final step for aligning the
 1309 model’s distilled knowledge with the specific formats and demands of downstream tasks.

1310 Table 14: Ablation for training recipe and teacher adapter fetch module. \dagger :Fail to follow instructions
 1311 (i.e., answer only single word).

Training Recipe	Teacher Adapter	Visual Question Answering				Compositional Reasoning				
		GQA	TextVQA	MME	Avg	Sugarcrape	SADE	BiVLC	Winoground	Avg
<i>Ablation on different training recipe</i>										
(1) PT + SFT	✓	57.9	50.6	61.2	56.6	73.3	63.9	58.5	47.2	60.7
(2) PT + DFT	✓	59.5	54.6	64.8	59.6	79.1	67.3	61.8	50.3	64.6
(3) DPT + SFT	✓	60.4	56.3	64.4	60.4	72.6	61.6	58.3	49.9	60.6
(4) DPT + DFT	✓	1.8 [†]	28.0 [†]	34.9 [†]	21.6 [†]	70.2	60.3	57.3	50.8	59.7
(5) DPT + SFT + DFT	✓	60.6	56.1	65.1	60.6	81.1	67.9	63.2	48.9	65.3
(*) DPT + DFT + SFT	✓	62.2	56.4	70.1	62.9	82.9	69.4	63.3	51.1	66.7

H.4 DETAILED EXPERIMENTS RESULTS ON SCALABILITY

H.4.1 DETAILED EXPERIMENTS RESULTS ON DATA SCALING

This section provides a detailed analysis of our experiments on scaling data quality and data quantity, with full results presented in Table 15. For a clear point of comparison, we also include the performance of a baseline model trained only with Supervised Fine-Tuning (SFT) on the same initial data volume.

Our findings clearly demonstrate the two-fold benefit of our approach. First, by using our distillation method, the model’s performance significantly improves over the SFT baseline, even with the same amount of data. This confirms that distillation provides a higher-quality training signal. Second, when we use more of this high-quality data (doubling the training samples), the model’s performance is further enhanced. These results validate that our distillation approach offers a substantial performance gain, which is then amplified by increasing the quantity of the training data. A detailed explanation of the training dataset configuration is provided in Appendix G.

Table 15: Data scaling experiment.

Student LLM	Teacher LLM	# Training Samples	Visual Question Answering				Compositional Reasoning				
			GQA	TextVQA	MME	Avg	Sugarcrape	SADE	BiVLC	Winoground	Avg
<i>Data scaling experiment</i>											
Qwen1.5-1.8B (SFT)		1.2 M	57.9	50.6	61.2	56.6	73.3	63.9	58.5	47.2	60.7
Qwen1.5-1.8B	Qwen1.5-4B	1.2 M	62.2	56.4	70.1	62.9	82.9	69.4	63.3	51.1	66.7
Qwen1.5-1.8B	Qwen1.5-4B	2.4 M	62.7	56.8	70.6	63.3	89.9	67.8	68.9	53.3	69.9

H.4.2 DETAILED EXPERIMENTS RESULTS ON STUDENT AND TEACHER LLM SIZE

This section provides a more detailed analysis of the relationship between teacher and student model sizes in our distillation framework, with full results presented in Table 16.

We first examine a 1.8B parameter student model. As the table shows, distilling from a larger 7B teacher yields a stronger student model compared to distilling from a 4B teacher, with improved performance on both VQA and CR tasks. It is worth noting that we selected a Qwen2.5-7B model as the larger teacher. This decision was made because preliminary evaluations showed that the performance of the Qwen1.5-7B model was not significantly higher than that of the Qwen1.5-4B version;

1350 using the more capable Qwen2.5 architecture ensured a more significant and meaningful gap in
 1351 teacher capacity for this experiment.

1352 This trend is further validated with a smaller, 0.5B parameter student. The results show a clear
 1353 progression: the 0.5B student first shows a dramatic improvement over its SFT-only baseline when
 1354 distilled from a 1.8B teacher. Performance increases again, and quite substantially, when the same
 1355 0.5B student is distilled from an even larger 4B teacher. This demonstrates that even smaller student
 1356 models can effectively absorb the enhanced capabilities of higher-capacity teachers.

1357 In summary, these experiments consistently show that a larger, more capable teacher model is a
 1358 critical factor in producing a stronger student, regardless of the student’s own size. A higher-capacity
 1359 teacher provides a richer and more effective source of knowledge, successfully transferring more
 1360 powerful reasoning abilities through our distillation process.

1362 Table 16: Student and teacher LLM Size experiment.

Student LLM	Teacher LLM	# Training Samples	Visual Question Answering				Compositional Reasoning			
			GQA	TextVQA	MME	Avg	Sugarcrape	SADE	BiVLC	Winoground
<i>Large teacher experiment</i>										
Qwen1.5-1.8B (SFT)	1.2 M		57.9	50.6	61.2	56.6	73.3	63.9	58.5	47.2
Qwen1.5-1.8B	Qwen1.5-4B	1.2 M	62.2	56.4	70.1	62.9	82.9	69.4	63.3	51.1
Qwen1.5-1.8B	Qwen2.5-7B	1.2 M	62.9	57.1	69.8	63.4	84.1	70.7	63.8	52.6
Qwen1.5-0.5B (SFT)	1.2 M		54.9	45.5	55.5	52.0	52.9	51.4	39.5	49.8
Qwen1.5-0.5B	Qwen1.5-1.8B	1.2 M	57.3	48.9	58.1	54.7	57.3	52.8	44.0	50.4
Qwen1.5-0.5B	Qwen1.5-4B	1.2 M	60.1	50.3	59.5	56.6	59.5	59.0	49.1	50.5
<i>Small teacher experiment</i>										
Qwen1.5-0.5B (SFT)	1.2 M		57.9	50.6	61.2	56.6	73.3	63.9	58.5	47.2
Qwen1.5-0.5B	Qwen1.5-4B	1.2 M	62.2	56.4	70.1	62.9	82.9	69.4	63.3	51.1
Qwen1.5-0.5B	Qwen2.5-7B	1.2 M	62.9	57.1	69.8	63.4	84.1	70.7	63.8	52.6
Qwen1.5-0.5B (SFT)	1.2 M		54.9	45.5	55.5	52.0	52.9	51.4	39.5	49.8
Qwen1.5-0.5B	Qwen1.5-1.8B	1.2 M	57.3	48.9	58.1	54.7	57.3	52.8	44.0	50.4
Qwen1.5-0.5B	Qwen1.5-4B	1.2 M	60.1	50.3	59.5	56.6	59.5	59.0	49.1	50.5

1371 H.4.3 DETAILED EXPERIMENTS RESULTS ON DIFFERENT LLM BACKBONES

1373 To verify the generalizability of our distillation framework, we conducted an experiment using an
 1374 entirely different architectural backbone, the MobileLLaMA (Chu et al., 2024) family. This section
 1375 provides a detailed analysis of these results, which are presented in the Table 17.

1376 Specifically, we applied our distillation method to a 1.4B parameter MobileLLaMA as the student
 1377 model, using a 2.7B parameter MobileLLaMA model as the teacher. We then compared its per-
 1378 formance to a baseline 1.4B student trained with only Supervised Fine-Tuning (SFT). The results
 1379 clearly show that our distillation method remains highly effective on this new architecture. The dis-
 1380 tillated student model significantly outperforms the SFT-only baseline across both Visual Question
 1381 Answering (VQA) and Compositional Reasoning (CR) benchmarks.

1382 This successful application demonstrates the robustness and architectural independence of our ap-
 1383 proach. It confirms that the core principles of our distillation method are not specifically tailored to
 1384 the Qwen (Qwen et al., 2025) model family but can be broadly applied to improve the performance
 1385 of different MLLM backbones, validating the generalizability of our findings.

1386 Table 17: Different LLM backbones experiment.

Student LLM	Teacher LLM	# Training Samples	Visual Question Answering				Compositional Reasoning			
			GQA	TextVQA	MME	Avg	Sugarcrape	SADE	BiVLC	Winoground
<i>Different LLM backbone experiment</i>										
MobileLLaMA-1.4B (SFT)	1.2M		53.3	43.8	52.2	49.7	50.1	50.0	37.5	37.5
MobileLLaMA-1.4B	MobileLLaMA-2.7B	1.2M	57.4	45.2	56.8	53.1	55.6	54.2	39.8	46.5

1394 I GENERALIZATION TO OTHER ARCHITECTURE

1397 To rigorously validate the robustness and generalizability of the proposed CompoDistill framework
 1398 beyond the LLaVA architecture, we extended our evaluation to the Qwen3-VL family.

1399 **Experimental Setup.** The Qwen3-VL architecture differs fundamentally from the LLaVA design
 1400 used in our main experiments. It incorporates distinct training schemes and advanced architectural
 1401 components, such as Native Resolution ViT (NaViT) and DeepStack. We conducted experiments
 1402 across varying model scales, ranging from 2B to 8B parameters, to assess scalability. For training
 1403 efficiency in these ablation studies, we utilized a 50% subset of the Cambrian737K dataset, with the
 1404 input resolution parameter `max_pixel_values` set to 32,768.

1404
1405
1406 Table 18: Different architecture experiment.
1407
1408
1409
1410
1411

Student LLM	Teacher LLM	Training Method	Visual Question Answering				Compositional Reasoning			
			GQA	TextVQA	MME	Avg	Sugarcrape	SADE	BiVLC	Avg
Qwen3-VL-2B	SFT	Naive KD	57.2	50.9	70.4	59.5	85.5	79.3	64.9	76.5
Qwen3-VL-4B	SFT	CompoDistill	59.7	56.7	80.0	65.5	91.6	84.4	67.2	81.1
Qwen3-VL-8B	SFT	CompoDistill	60.0	58.2	80.9	66.4	93.0	85.5	68.1	82.2
Qwen3-VL-2B	Qwen3-VL-4B	Naive KD	58.9	55.3	72.1	62.1	86.2	79.6	65.8	77.2
Qwen3-VL-2B	Qwen3-VL-4B	CompoDistill	59.4	58.9	73.2	63.8	91.0	81.4	67.1	79.8
Qwen3-VL-2B	Qwen3-VL-8B	CompoDistill	59.5	59.2	73.7	64.1	91.5	81.5	67.4	80.1

1412
1413
1414 **Results and Analysis.** Table 18 presents the performance comparison on Visual Question An-
1415 swering (VQA) and Critical Reasoning (CR) tasks. Despite the structural differences in the vision
1416 encoder and language model, CompoDistill consistently demonstrates strong performance improve-
1417 ments. This confirms that the visual attention misalignment bottleneck is not specific to LLaVA
1418 but is a broader phenomenon in MLLMs, and that our multi-stage distillation strategy generalizes
1419 effectively to diverse architectures and larger model scales.

1420 J DISCUSSION ABOUT TRAINING OVERHEAD

1421 In this section, we provide a comprehensive analysis of the computational efficiency of our pro-
1422 posed framework, CompoDistill, compared to existing state-of-the-art knowledge distillation (KD)
1423 methods.

1424 **Quantitative Comparison.** Table 19 summarizes the training overhead of our method against
1425 other baselines, LLaVA-KD and LLaVA-MoD. Our framework requires significantly fewer training
1426 hours compared to the baselines while maintaining a comparable number of training stages. Specifically,
1427 the total training time of CompoDistill is approximately **170 hours** (consisting of DPT: 28h,
1428 DFT: 88h, and SFT: 54h), which is substantially faster than LLaVA-KD (\sim 320 hours) and LLaVA-
1429 MoD (\sim 960 hours).

1430 Table 19: Comparison of training overhead between our method and existing baselines. Our method
1431 achieves the lowest total training time with streamlined loss components.

Method	Training Stages	Loss Components	Total Training Time (hrs)
LLaVA-KD	3 stages	4 losses	\sim 320
LLaVA-MoD	4 stages	3 losses	\sim 960
CompoDistill	3 stages	3 losses	\sim 170

1440
1441
1442 **Computational Complexity Analysis.** The efficiency of our method stems from the design of the
1443 distillation objectives. **LLaVA-KD** introduces a significant computational bottleneck by calculating
1444 an expensive correlation matrix for all visual tokens between the student and teacher, resulting in
1445 a complexity of $\mathcal{O}(N_v^2 \times d)$, where N_v is the number of visual tokens and d is the hidden dimen-
1446 sion. Similarly, the extended training time of **LLaVA-MoD** is attributed to the complex routing and
1447 computation within its Mixture of Experts (MoE) architecture. In contrast, our VAT attention loss
1448 in **CompoDistill** operates with a much lower time complexity of $\mathcal{O}(N_v \times L)$, where L denotes the
1449 number of layers. This linear complexity with respect to visual tokens allows for highly efficient
1450 training without sacrificing performance.

1451
1452 **Resource-Constrained Settings.** To further address practicality under resource-constrained en-
1453 vironments, the memory overhead of our multi-module framework can be effectively mitigated.
1454 Since the teacher model is static during distillation, its outputs (logits and attention maps) can be
1455 pre-computed and stored offline. This strategy decouples the teacher’s memory requirement from
1456 the student’s training loop, allowing our method to be deployable on GPUs with limited VRAM
1457 capacity.

1458 **K ADDITIONAL EXPERIMENT ON ATTENTION MIXING**
14591460 In this section, we investigate the causal relationship between the similarity of visual attention to
1461 the teacher model and the performance on vision-centric tasks. While our main paper (Figure 4 in
1462 Sec 3.3) suggests this correlation, we conducted additional ablation studies to empirically verify that
1463 the performance gain primarily originates from the distilled teacher’s *visual* attention.
14641465 **Experimental Setup.** We extended the experimental setup from Sec 3.3 by introducing three variations
1466 of attention mixing strategies during inference. Keeping all other conditions identical, we
1467 compared the following settings:
14681469

- **LLaVA-KD:** The baseline method.
- + **Teacher Visual Attention (Ours):** Incorporating visual attention from the distilled teacher
(Qwen1.5-4B based).
- + **Teacher Text Attention:** Using the teacher’s text attention instead of visual attention.
- + **Other Visual Attention:** Using visual attention from a larger, external MLLM (Qwen1.5-7B)
to test if simply using a stronger model suffices.
- + **Random:** Injecting random attention maps as a control.
- + **Teacher Attention:** Using both the teacher’s visual and text attention.

14701471 **Quantitative Results.** Table 20 presents the accuracy scores across three compositional reasoning
1472 tasks: Swap, Replace, and Add.
14731474 Table 20: Different architecture experiment.
14751476

	Method # Data Num	Swap 912	Replace 3,846	Add 2,754
(a)	LLaVA-KD	0.6218	0.8023	0.8435
(b)	+ Teacher Visual Attention (Ours)	0.6419	0.8140	0.8747
(c)	+ Teacher Text Attention	0.6157	0.8045	0.8535
(d)	+ Other Visual Attention (Qwen1.5-7B)	0.6354	0.8059	0.8567
(e)	+ Random	0.2094	0.1708	0.1959
(f)	+ Teacher Attention (Visual + Text)	0.6360	0.8210	0.8531

1477 **Analysis.** The results provide clear empirical support for our framework design. First, utilizing the
1478 teacher’s visual attention (b) consistently outperforms the baseline (a) across all datasets, confirming
1479 that visual attention is the key driving factor. This is further corroborated by the comparison between
1480 (b) and (c), which reveals that unlike visual attention, text attention does not yield similar improve-
1481 ments for vision-centric tasks. Second, a critical observation arises from the comparison between (b)
1482 and (d), demonstrating that alignment is more critical than mere model power. Although the external
1483 model (Qwen1.5-7B) is significantly more powerful than our teacher (Qwen1.5-4B), simply mixing
1484 its attention fails to achieve optimal performance. This indicates that attention alignment is effective
1485 only when the student and teacher feature spaces are intrinsically aligned.
14861487 In conclusion, these experiments justify the design of our VAT and TAF modules, confirming that
1488 precise alignment with the teacher’s visual attention is a requisite for improving compositional rea-
1489 soning capabilities.
14901491 **L ADDITIONAL EXPERIMENT ON TEACHER ADAPTER FETCH MODULE**
14921493 In this section, we address the potential concern that reusing the frozen teacher adapter (Teacher
1494 Adapter Fetch, TAF) might constrain the student’s flexibility or lock it into the teacher’s visual-
1495 linguistic idiosyncrasies. We compare our approach against training a student-side adapter from
1496 scratch to clarify the trade-offs between efficiency and adaptability.
14971498 **On the Lock-in Effect.** We first clarify that the primary goal of our framework is to faithfully
1499 distill the teacher’s rich visual capabilities into an efficient student model. Since both models share
1500 the same SFT and KD data, mimicking the teacher’s generation behavior is a deliberate design
1501

choice to maximize capability transfer rather than a limitation. As supported by prior distillation studies, accurate alignment with the teacher often enhances the student’s generalization rather than restricting it.

Comparative Experiment: Student-Side Adapter Training. To empirically validate the effectiveness of TAF, we conducted a comparative experiment against a Student-Side-Match approach.

- **Setup:** Instead of reusing the teacher’s frozen adapter, we initialized a new vision adapter on the student side and trained it to align with the teacher’s representation space. This process required an additional training stage using the LLaVA-1.5-558K dataset before proceeding to the DPT, DFT, and SFT stages.

- **Overhead:** We note that this explicit alignment strategy introduced significant computational overhead, requiring approximately **40 additional training hours**.

Results and Analysis. Table 21 compares the performance of the Baseline (SFT), the Student-Side-Match method, and our proposed CompoDistill (TAF). As shown in the results, our TAF module consistently outperforms the Student-Side-Match approach. This demonstrates that reusing the teacher’s adapter is not only more computationally efficient but also provides a more effective mechanism for aligning the student’s visual space with the teacher’s, without compromising adaptability to the target tasks.

Table 21: Comparison of training strategies with computational overhead.

Student MLLM	Method	Teacher	Extra Time	VQA				CR			
				GQA	TextVQA	MME	Avg	Winoground	SugarCrepe	BiVLC	Avg
Qwen1.5-1.8B	SFT	-	-	57.9	50.6	61.2	54.9	47.2	73.3	58.5	59.7
Qwen1.5-1.8B	Student-Side-Match	Qwen1.5-4B	+40h	56.8	52.3	68.5	59.2	50.6	78.2	60.8	63.2
Qwen1.5-1.8B	TAF (Ours)	Qwen1.5-4B	+0h	62.2	56.4	70.1	61.9	51.2	82.9	63.3	65.8

M ADDITIONAL EXPERIMENT ON VISUAL ATTENTION ALIGNMENT MODULE

In this section, we investigate the impact of updating attention parameters during the distillation process. Specifically, we address the hypothesis that freezing attention blocks in the middle layers while only updating Feed-Forward Networks might help mitigate potential over-mimicry or improve generalization.

Experimental Validation: Freezing vs. Tuning. To empirically verify the necessity of attention tuning, we conducted a comparative experiment with two settings:

- **Freeze:** Freezing the parameters of the attention blocks in the middle layers and updating only the FFNs.
- **Tuning (Ours):** Updating both attention blocks and FFNs as proposed in our VAT module.

Results and Analysis. Table 22 presents the performance comparison on VQA and Critical Reasoning (CR) tasks. As shown in the results, freezing the attention blocks leads to a consistent performance degradation across all metrics compared to our standard setting. We interpret this as evidence that the self-attention mechanism is critical for learning the visual reasoning process. Restricting the update of attention parameters acts as a bottleneck, preventing the student from effectively learning the spatial relationships and where to look required for complex visual tasks. This confirms that adapting the attention mechanism is essential for successfully distilling the teacher’s visual capabilities.

N DISCUSSION ON POSSIBILITY ABOUT TEACHER OVERFITTING

1566 Table 22: Impact of Attention Block tuning in the Visual Attention Alignment (VAT) module.
1567

Student	Teacher	Attention Block Strategy	VQA				CR		
			GQA	TextVQA	MME	Avg	Winoground	SugarCrepe	BiVLC
Qwen1.5-1.8B	Qwen1.5-4B	Freeze	61.6	55.9	64.6	60.7	49.4	80.4	62.9
Qwen1.5-1.8B	Qwen1.5-4B	Tuning (Ours)	62.2	56.4	70.1	61.9	51.2	82.9	63.3

1571
1572
1573 In this section, we address the concern regarding the risk of the student model strictly overfitting
1574 to the teacher’s visual focus patterns, which might dampen exploration or degrade robustness. We
1575 provide both empirical evidence and a discussion on our loss function design to demonstrate that
1576 CompoDistill encourages intrinsic visual reasoning rather than brittle mimicry.
1577

1577 **Empirical Analysis of Focus Patterns.** To verify whether the student merely mimics the teacher
1578 or acquires an intrinsic ability to discern where to look, we analyzed the relationship between at-
1579 tention alignment and task performance using the SugarCrepe dataset. We stratified the test samples
1580 based on the visual attention similarity between the teacher and student at visual understanding
1581 layers.
1582

1582 Table 23 summarizes the performance and data distribution across different similarity intervals. We
1583 observe two key trends:
1584

- **Absence of Over-fitting:** The majority of samples (55.5%) are concentrated in the moderate sim-
1585 ilarity range of [0.6, 0.7), rather than clustering in the highest similarity intervals (e.g., [0.9, 1.0]).
1586 This distribution indicates that the student does not simply mimic the teacher’s attention map but
1587 learns a generalized representation.
1588
- **Robust Intrinsic Reasoning:** Notably, CompoDistill maintains strong performance (0.76) even
1589 in intervals where attention similarity is relatively low ([0.5, 0.6)). This implies that the student
1590 has acquired robust visual reasoning capabilities, enabling it to derive correct answers even when
1591 its visual focus partially deviates from that of the teacher.
1592

1593 Table 23: Analysis of performance and sample distribution relative to Attention Similarity.
1594

Similarity Range	[0.5, 0.6)	[0.6, 0.7)	[0.7, 0.8)	[0.8, 0.9)	[0.9, 1.0]
Performance	0.76	0.87	0.82	0.79	0.82
Data distribution	5.5%	55.5%	15.0%	11.6%	12.4%

1595
1596
1597
1598
1599
1600 **Design Choice of VAT Loss Function.** Furthermore, our specific choice of **Cosine Similarity** for
1601 the Visual Attention Alignment (VAT) loss is a deliberate design decision to mitigate overfitting.
1602 In our preliminary ablation studies, we observed that stricter alignment objectives, such as Mean
1603 Squared Error (MSE) or KL Divergence, led to performance degradation in VQA tasks.
1604

1605 We attribute this to the nature of the loss functions: while MSE forces the student to match the ab-
1606 solute magnitude of the teacher’s values (encouraging point-to-point mimicry), Cosine Similarity
1607 aligns the *direction* of the attention vectors. This approach teaches the student the *relative impor-*
1608 *tance* of visual tokens without enforcing rigid adherence to the teacher’s exact distribution, thereby
1609 fostering the learning of underlying reasoning patterns while preserving robustness.
1610

1611 O ADDITIONAL EXPERIMENT ON VISUAL GROUNDING 1612

1613 In this section, we empirically validate the impact of the Visual Attention Alignment (VAT) mod-
1614 ule on localization (grounding) capabilities. Given that CompoDistill demonstrates superior per-
1615 formance in fine-grained visual-centric tasks (e.g., Compositional Reasoning and Hallucination
1616 mitigation), we hypothesized that the improved visual attention alignment would naturally extend to
1617 precise visual grounding.
1618

1619 **Experimental Setup.** We evaluated the models on the RefCOCO benchmark. To ensure a fair
1620 comparison, all models, including the baselines (SFT and LLaVA-KD), utilized Qwen1.5-1.8B as
1621 the backbone LLM. Performance is measured using the Accuracy@0.5 (Acc@0.5) metric.
1622

1620
 1621 **Results and Analysis.** Table 24 presents the quantitative results. Our proposed method, Compo-
 1622 Distill, significantly outperforms both the SFT baseline and the LLaVA-KD method. Specifically,
 1623 CompoDistill achieves an accuracy of **57.8%**, representing a substantial improvement over LLaVA-
 1624 KD (45.4%). This empirical evidence confirms that the fine-grained visual attention alignment pro-
 1625 vided by VAT not only improves reasoning capabilities but also translates effectively to precise
 object localization.

1626 Table 24: Performance comparison on the visual grounding task (RefCOCO-val).
 1627

Method	Backbone LLM	RefCOCO-val (Acc@0.5)
SFT	Qwen1.5-1.8B	16.2
LLaVA-KD	Qwen1.5-1.8B	45.4
CompoDistill (Ours)	Qwen1.5-1.8B	57.8

P LIMITATION AND FUTURE WORK

1634 A potential limitation of CompoDistill lies in its inability to capture the distinct information carried
 1635 by each head within multi-head attention (Zhao et al., 2024; Kang et al., 2025), as it distills only the
 1636 average of the teacher’s visual attention across all heads. This simplification may lead to information
 1637 loss by overlooking the diverse roles played by individual heads. Moreover, CompoDistill assumes
 1638 that the teacher and student MLLMs belong to the same LLM series, as consistency in vocabulary is
 1639 required for logit-based distillation (Equation 4 in the main paper). This constraint poses a challenge
 1640 when attempting to distill visual knowledge from teachers belonging to different model families.
 1641

1642 As future work, we aim to incorporate the head-specific characteristics of the teacher’s visual at-
 1643 tention into the distillation process, enabling the student to capture more fine-grained and nuanced
 1644 visual cues.
 1645

1646
 1647
 1648
 1649
 1650
 1651
 1652
 1653
 1654
 1655
 1656
 1657
 1658
 1659
 1660
 1661
 1662
 1663
 1664
 1665
 1666
 1667
 1668
 1669
 1670
 1671
 1672
 1673